Probability of Resolution of MUSIC and g-MUSIC: An Asymptotic Approach

David Schenck*, Xavier Mestre†, and Marius Pesavento*
*Communication Systems Group, Technische Universität Darmstadt, Germany
†Centre Tecnològic de Telecomunicacions de Catalunya, Castelldefels, Spain

***Abstract*—In this article, the outlier production mechanism of the conventional Multiple Signal Classification (MUSIC) and the g-MUSIC Direction-of-Arrival (DoA) estimation technique is investigated using tools from Random Matrix Theory (RMT). A general Central Limit Theorem (CLT) is derived that allows to analyze the asymptotic stochastic behavior of eigenvector-based cost functions in the asymptotic regime where the number of snapshots and the number of antennas increase without bound at the same rate. Furthermore, this CLT is used to provide an accurate prediction of the resolution capabilities of the MUSIC and the g-MUSIC DoA estimation method. The finite dimensional distribution of the MUSIC and the g-MUSIC cost function is shown to be asymptotically jointly Gaussian distributed in this asymptotic regime.**

***Index Terms*—MUSIC, g-MUSIC, DoA estimation, central limit theorem, random matrix theory, probability of resolution, performance analysis.**

I. Introduction

Due to the vast variety of use cases, DoA estimation belongs to the most relevant research areas in signal processing. The applications range from radar and sonar to electric surveillance, seismology, astronomy and mobile communications [1]–[4]. Multiple DoA estimation techniques have been proposed in the literature. Among them, subspace-based DoA estimation techniques which are known to provide a good compromise between computational complexity and DoA estimation accuracy. This is mainly because these methods avoid multidimensional searches while providing relatively good performance. One of the most popular examples of subspace-based DoA estimation methods is MUSIC [5], which exploits the orthogonality between signal and noise subspaces by finding the DoAs that achieve the highest orthogonality between the array signature and the noise subspace of the sample covariance matrix. It was recently recognized [6] that the noise space spanned by the sample covariance matrix is not a consistent estimate of the true one when both the sample size and the number of array elements become large but are still comparable in magnitude. Therefore, it is possible to come up with a refined MUSIC algorithm, usually referred to as g-MUSIC [6], which replaces the noise sample eigenvectors by a consistent estimate of the true noise subspace. This provides a significant improvement in terms of both accuracy and resolution in the low sample size scenario, whereby the number of snapshots and the number of array elements have the same order of magnitude. In any case, both MUSIC and g-MUSIC are subspaced-based algorithms, and as such both suffer from the so-called breakdown or threshold effect. This effect is characterized by a rapid loss of resolution capabilities when either the sample size (in snapshots per antenna) or the Signal-to-Noise Ratio (SNR) falls below a certain value. When this occurs, the DoA of one of the sources is estimated as an outlier, which leads to a complete breakdown in terms of accuracy [7].

The objective of this paper is to analytically characterize this breakdown effect in both DoA estimation algorithms. More specifically, we investigate the probability that these algorithms resolve two close sources in the asymptotic regime where both the sample size and the number of array elements tends to infinity at the same rate. Up to now, the literature has mainly focused on the performance characterization of the conventional MUSIC method in terms of both accuracy and resolution probability [8]–[14]. Most of the performance analyses rely on conventional large sample-size asymptotics, where the number of array elements is assumed to be fixed while the number of snapshots grows without bound. This asymptotic regime is not very suitable for characterizing the threshold performance, since loss of resolution occurs e.g. when the number of snapshots is not much larger (or even smaller) than the number of antennas. For this reason, we propose here to analyze this outlier production mechanism under the more realistic setting where these two quantities are large but comparable in magnitude. This is indeed the setting that was considered in [15] to investigate the consistency of the DoA estimates obtained through MUSIC or g-MUSIC.

We extend the work in [15] and analyze the statistical fluctuations of the MUSIC and g-MUSIC cost functions, which are the key to understanding the outlier production mechanism that leads to loss of resolution. The approach is similar to the one followed in [16]–[18] to study the resolution capabilities of the recently introduced Partially Relaxed Deterministic Maximum Likelihood (PR-DML) algorithm. It also shares some ideas with [19], [20], where the resolution probability of the conventional Deterministic Maximum Likelihood (DML) and the Stochastic Maximum Likelihood (SML) method are derived through an asymptotic characterization of stochastic fluctuations of the corresponding multidimensional cost functions. In comparison to the PR-DML, DML and SML cost functions, the MUSIC and g-MUSIC cost functions involve eigenvectors of a random matrix and therefore require a fundamentally new asymptotic analysis. Furthermore, eigenvector-based cost functions are shown to be asymptotically jointly Gaussian distributed and a general CLT is provided that allows to characterize the asymptotic fluctuations of such cost functions. The asymptotic second order behavior is expressed as a double contour integral which is solved for both MUSIC

Parts of this work were published at *IEEE International Conference on Acoustics, Speech, and Signal Processing (ICASSP 2021).*

and g-MUSIC. Finally, the derived asymptotic distribution of both cost functions is used to predict the probability of resolution of both subspace-based DoA estimation methods. In comparison to [21], we do not only analyze the asymptotic stochastic behavior of the g-MUSIC cost function but also of the conventional MUSIC cost function. Additionally, the detailed proofs for the second order asymptotic behavior of both cost functions are provided.

The original contributions of this article can be summarized as follows:

- We derive a CLT which states that eigenvector-based cost functions are asymptotically jointly Gaussian distributed for Gaussian distributed observations in the asymptotic regime where both sample size and array dimension go to infinity at the same rate. A general theorem is provided that completely specifies the asymptotic behavior of eigenvector-based cost functions in terms of (i) asymptotic deterministic behavior and (ii) fluctuations around this deterministic equivalent.
- We determine a set of conditions that guarantee that both MUSIC and g-MUSIC cost functions fluctuate around their asymptotic deterministic equivalents in this asymptotic regime.
- We particularize the above results to the MUSIC and g-MUSIC cost functions and derive a closed-form expression for the asymptotic probability of resolution of both DoA estimation methods. These expressions can be used to determine the probability of resolving closely spaced sources for a given array geometry, a sample volume per antenna and a scenario configuration.

The rest of the paper is organized as follows. Section II introduces the signal model that is assumed in the paper, while some important RMT fundamentals are then introduced in Section III. The conventional MUSIC and g-MUSIC DoA estimation techniques are presented in Section IV. The asymptotic stochastic analysis of these two cost functions and the corresponding probability of resolution of the associated methods are given in Section V. Section VI is devoted to the derivation of the asymptotic deterministic behavior of these two cost functions and the characterization of the corresponding fluctuations around it. Finally, these theoretical derivations are then validated by numerical experiments in Section VII and Section VIII concludes the paper.

II. Signal Model

Consider a sensor array that is equipped with M sensors and K impinging narrowband signals with DoAs $\boldsymbol{\theta}=[\theta_1,...,\theta_K]^{\mathrm{T}}$ that lie within the field of view Θ of the array. The number of sources K is assumed to be known and smaller than the number of sensors $K<M$. The full-rank steering matrix is given by $\boldsymbol{A}(\boldsymbol{\theta})=[\boldsymbol{a}(\theta_1),...,\boldsymbol{a}(\theta_K)]^{\mathrm{T}}\in\mathbb{C}^{M\times K}$ where $\boldsymbol{a}(\theta_i)\in\mathbb{C}^M$ denotes the steering vector associated to the i-th source, which is assumed to be located at θ_i. Without loss of generality, we will assume that the array steering vector is normalized to have unit norm, that is $\|\boldsymbol{a}(\theta)\|=1$. The received baseband signal $\boldsymbol{y}(n)=[y_1(n),...,y_M(n)]^{\mathrm{T}}\in\mathbb{C}^M$ at time instant n is modeled as:

$$\boldsymbol{y}(n)=\boldsymbol{A}(\boldsymbol{\theta})\boldsymbol{s}(n)+\boldsymbol{n}(n) \text{ for } n=1,...,N \tag{1}$$

where $\boldsymbol{s}(n)=[s_1(n),...,s_K(n)]^{\mathrm{T}}\in\mathbb{C}^K$ denotes the transmitted baseband source signal and $\boldsymbol{n}(n)$ represents the sensor noise. Assuming that both signal and noise vectors are statistically independent, zero-mean and circularly symmetric Gaussian vectors, the observation $\boldsymbol{y}(n)$ in (1) can be modeled as a zero-mean circularly symmetric Gaussian vector with covariance matrix $\boldsymbol{R}\in\mathbb{C}^{M\times M}$ given by

$$\boldsymbol{R}=\mathbb{E}\left[\boldsymbol{y}(n)\boldsymbol{y}(n)^{\mathrm{H}}\right]=\boldsymbol{A}\boldsymbol{R}_{\mathrm{s}}\boldsymbol{A}^{\mathrm{H}}+\sigma^2\boldsymbol{I}_M \tag{2}$$

where $\boldsymbol{R}_{\mathrm{s}}=\mathbb{E}[\boldsymbol{s}(n)\boldsymbol{s}(n)^{\mathrm{H}}]\in\mathbb{C}^{K\times K}$ is the covariance matrix of the transmitted source signal $\boldsymbol{s}(n)$ and $\sigma^2\boldsymbol{I}_M$ denotes the noise covariance. Let us consider the eigendecomposition of this covariance matrix, which can be expressed as

$$\boldsymbol{R}=\sum_{m=1}^{\bar{M}}\gamma_m\boldsymbol{E}_m\boldsymbol{E}_m^{\mathrm{H}}=\boldsymbol{E}\begin{bmatrix}\gamma_1\boldsymbol{I}_{K_1} & & \\ & \ddots & \\ & & \gamma_{\bar{M}}\boldsymbol{I}_{K_{\bar{M}}}\end{bmatrix}\boldsymbol{E}^{\mathrm{H}}. \tag{3}$$

Here, $\bar{M}\leq M$ denotes the total number of distinct eigenvalues, which are sorted in ascending order as $\gamma_1<\gamma_2<\cdots<\gamma_{\bar{M}}$, and K_m denotes the multiplicity of γ_m, $m=1,...,\bar{M}$. The eigenvectors associated to γ_m are grouped into an $M\times K_m$ matrix $\boldsymbol{E}_m$ of orthogonal columns that span the corresponding subspace and we let $\boldsymbol{E}=[\boldsymbol{E}_1,...,\boldsymbol{E}_{\bar{M}}]\in\mathbb{C}^{M\times M}$.

We also consider here the sample covariance matrix

$$\hat{\boldsymbol{R}}=\frac{1}{N}\sum_{n=1}^{N}\boldsymbol{y}(n)\boldsymbol{y}(n)^{\mathrm{H}}=\frac{1}{N}\boldsymbol{Y}\boldsymbol{Y}^{\mathrm{H}} \tag{4}$$

which has eigendecomposition given by

$$\hat{\boldsymbol{R}}=\sum_{m=1}^{M}\hat{\lambda}_m\hat{\boldsymbol{e}}_m\hat{\boldsymbol{e}}_m^{\mathrm{H}}=\hat{\boldsymbol{E}}\begin{bmatrix}\hat{\lambda}_1 & & \\ & \ddots & \\ & & \hat{\lambda}_M\end{bmatrix}\hat{\boldsymbol{E}}^{\mathrm{H}} \tag{5}$$

where now $\hat{\lambda}_1\leq\hat{\lambda}_2\leq\cdots\leq\hat{\lambda}_M$ are the sample eigenvalues, $\hat{\boldsymbol{e}}_m$ denotes the eigenvector associated to $\hat{\lambda}_m$, $m=1,...,M$ and $\hat{\boldsymbol{E}}=[\hat{\boldsymbol{e}}_1,...,\hat{\boldsymbol{e}}_M]$. These sample eigenvalues are almost surely different, unless $N<M$, in which case we have a zero sample eigenvalue of multiplicity $M-N$. In this situation, $\hat{\boldsymbol{e}}_m$ for $m=1,...,M-N$, span the subspace associated to the zero sample eigenvalue. In the following section, we provide some interesting properties of the asymptotic behavior of sample eigenvalues and eigenvectors based on RMT results that will be extensively used throughout the paper.

III. Random Matrix Theory Preliminaries

Under the above statistical assumptions, the sample covariance matrix $\hat{\boldsymbol{R}}$ in (4) is a consistent estimator of the true one $\boldsymbol{R}$, provided that the number of antennas M is kept fixed while the number of samples grows without bound, $N\to\infty$. More formally, one can easily show that $\|\hat{\boldsymbol{R}}-\boldsymbol{R}\|\to 0$ with probability one under these asymptotic assumptions, where here $\|\cdot\|$ denotes spectral norm. As pointed out before, this asymptotic regime is often unrealistic in the sense that both M,N are typically comparable in magnitude. In this paper, we will therefore consider an asymptotic regime where these two quantities tend to infinity at the same rate.

Assumption 1. *The number of samples N is a function of the number of antennas M, that is $N=N(M)$ and $N(M)\to\infty$ as $M\to\infty$ in a way that $M/N(M)\to c$ for some constant $0<c<\infty$.*

It turns out that under Assumption 1 the sample covariance matrix $\hat{\boldsymbol{R}}$ in (4) is not a consistent estimate of the true one in (2), in the sense that $\|\boldsymbol{R}-\hat{\boldsymbol{R}}\|\nrightarrow 0$. In particular, this shows that the eigenvalues and eigenvectors of $\hat{\boldsymbol{R}}$ do not really converge to the eigenvalues and eigenvectors of $\boldsymbol{R}$ when the dimensions of these matrices increase without bound. However, it is well known that, under some additional assumptions, the empirical eigenvalue distribution of the sample covariance matrix $\hat{\boldsymbol{R}}$ in (4) still shows a deterministic behavior in the large-dimensional regime. In order to formalize this observation, we need to introduce some additional technical assumptions.

Assumption 2. *The observations $\boldsymbol{y}(n)$ in* (1)*, $n{=}1,...,N$ form a collection of independent circularly symmetric complex Gaussian vectors with zero-mean and covariance matrix $\boldsymbol{R}$, bounded in spectral norm. In particular, the quantities $\bar{M}$, $\gamma_1,...,\gamma_{\bar{M}}$ and $K_1,...,K_{\bar{M}}$ corresponding to the eigendecomposition of $\boldsymbol{R}$ in* (3) *may vary with M, but $\sup_M \gamma_{\bar{M}}{<}\infty$.*

Under the above technical assumptions, the eigenvalues of the sample covariance matrix $\hat{\boldsymbol{R}}$ in (4) are asymptotically almost surely distributed as a non-random measure with density $q_M(x)$ [22]–[25]. Informally stated, the histogram of the eigenvalues of the sample covariance matrix tends to be shaped around $q_M(x)$ as M,N grow large, with probability one. This deterministic density is therefore the key to understanding the asymptotic behavior of the sample covariance matrix. In particular, one can show that, when $N{>}M$, the density $q_M(x)$ has compact support consisting of the union of S closed intervals, namely $\mathcal{S}{=}[x_1^-,x_1^+]\cup\cdots\cup[x_S^-,x_S^+]$ [24], [26], [27]. When $N{\le}M$, the same description is valid but with the addition of the zero eigenvalue, i.e. $\{0\}$. The procedure to obtain $\mathcal{S}$ is as follows (see [25, Proposition 1] and also [26]). Consider the following function of the true covariance matrix

$$\Psi(\omega){=}\frac{1}{N}\mathrm{tr}\left[\boldsymbol{R}^2(\boldsymbol{R}{-}\omega\boldsymbol{I}_M)^{-2}\right]. \tag{6}$$

The polynomial equation $\Psi(\omega){=}1$ has $2S$ solutions counting multiplicities, which can be denoted as $\{\omega_1^-,\omega_1^+,...,\omega_S^-,\omega_S^+\}$. We then define $x_s^\pm{=}z(\omega_s^\pm)$, $s{=}1,...,S$, where $z(\omega)$ is the transformation

$$z(\omega){=}\omega\left(1{-}\frac{1}{N}\mathrm{tr}\left[\boldsymbol{R}(\boldsymbol{R}{-}\omega\boldsymbol{I}_M)^{-1}\right]\right). \tag{7}$$

Each eigenvalue of $\boldsymbol{R}$ can be univocally associated to one of the S intervals, in the sense that there exists a single interval $[\omega_s^-,\omega_s^+]$ that contains that particular eigenvalue. On the other hand, given a certain covariance matrix $\boldsymbol{R}$, the number of intervals of the support S increases with increasing N. Furthermore, there exists a minimum number of samples per antenna that guarantees that a certain interval $[x_s^-,x_s^+]$ is associated to a single eigenvalue of $\boldsymbol{R}$. In this paper, we will strongly rely on the assumption that the lowest eigenvalue of $\boldsymbol{R}$ is the only eigenvalue that belongs to the interval $[\omega_1^-,\omega_1^+]$ (see Assumption 3 below). This will allow us to analyze the behavior of subspace DoA detection techniques in large dimensional arrays.

Having reviewed some basic notions on the asymptotic spectral behavior of the sample covariance matrix, we are now in the position of introducing the MUSIC and g-MUSIC subspace DoA estimators in the large antenna regime.

IV. MUSIC and g-MUSIC Direction-of-Arrival Estimation

The main idea behind the conventional MUSIC estimator is to exploit the fact that the eigenvectors associated to the noise subspace $\boldsymbol{E}_1$ of the true covariance matrix $\boldsymbol{R}$ in (3) are orthogonal to the steering vectors evaluated at the true DoAs of the received signals. Hence, we can consider a cost function

$$\bar{\eta}_{\mathrm{g}}(\theta){=}\boldsymbol{a}(\theta)^{\mathrm{H}}\boldsymbol{E}_1\boldsymbol{E}_1^{\mathrm{H}}\boldsymbol{a}(\theta). \tag{8}$$

where we recall from (3) that $\boldsymbol{E}_1$ contains the $M{-}K$ eigenvectors associated to the smallest eigenvalue of $\boldsymbol{R}$. The DoAs of the received signals can be determined as the K distinct values of θ at which $\bar{\eta}_{\mathrm{g}}(\theta){=}0$ [6]. Since the noise subspace $\boldsymbol{E}_1$ is unknown in practice, the conventional MUSIC cost function is obtained by replacing the noise subspace $\boldsymbol{E}_1$ in (8) with the noise eigenvectors of the sample covariance matrix, namely

$$\hat{\eta}_{\mathrm{c}}(\theta){=}\boldsymbol{a}(\theta)^{\mathrm{H}}\sum_{m=1}^{M-K}\hat{\boldsymbol{e}}_m\hat{\boldsymbol{e}}_m^{\mathrm{H}}\boldsymbol{a}(\theta) \tag{9}$$

and the DoAs are determined by the K distinct values in θ where $\hat{\eta}_{\mathrm{c}}(\theta)$ in (9) attains its K deepest local minima [5].

Now, as a consequence of the fact that under Assumption 2 $\|\boldsymbol{R}{-}\hat{\boldsymbol{R}}\|\nrightarrow 0$ one can generally expect that $|\hat{\eta}_{\mathrm{c}}(\theta){-}\eta_{\mathrm{g}}(\theta)|\nrightarrow 0$. With the help of RMT tools, one can however find a modification of the MUSIC cost function in (9) that is indeed consistent in this large dimensional regime. This is usually referred to as M,N-consistency, as opposed to the more conventional concept of N-consistency, which assumes a constant M. The modified cost function is usually referred to as g-MUSIC [6] and can be built from a proper combination of signal and noise subspaces, that is

$$\hat{\eta}_{\mathrm{g}}(\theta){=}\sum_{m=1}^{M}\phi(m)\boldsymbol{a}(\theta)^{\mathrm{H}}\hat{\boldsymbol{e}}_m\hat{\boldsymbol{e}}_m^{\mathrm{H}}\boldsymbol{a}(\theta) \tag{10}$$

with real-valued weights

$$\phi(m){=}\begin{cases}1{+}\sum_{k=M-K+1}^{M}\left(\frac{\hat{\lambda}_k}{\hat{\lambda}_m-\hat{\lambda}_k}-\frac{\hat{\mu}_k}{\hat{\lambda}_m-\hat{\mu}_k}\right), & m{\le}M{-}K\\ -\sum_{k=1}^{M-K}\left(\frac{\hat{\lambda}_k}{\hat{\lambda}_m-\hat{\lambda}_k}-\frac{\hat{\mu}_k}{\hat{\lambda}_m-\hat{\mu}_k}\right), & m{>}M{-}K\end{cases}$$

where $\hat{\mu}_1{\le}\hat{\mu}_2{\le}\cdots{\le}\hat{\mu}_M$ are the real-valued solutions (counting multiplicities) to the following equation in $\hat{\mu}$

$$\frac{1}{N}\sum_{k=1}^{M}\frac{\hat{\lambda}_k}{\hat{\lambda}_k{-}\hat{\mu}}{=}1.$$

The DoAs of the g-MUSIC estimator are determined by searching for the K deepest local minima of the cost function $\hat{\eta}_{\mathrm{g}}(\theta)$ in (10). In order to justify the superiority of this DoA estimation algorithm, we need to impose separation between the signal and noise subspaces in the asymptotic covariance $\boldsymbol{R}$. This is more formally stated in the following assumption.

Assumption 3. *We have $0{<}\inf_M K_1/M{\le}\sup_M K_1/M{<}1$ and $\inf_M\gamma_1{>}0$. The eigenvalue γ_1 is the unique eigenvalue that is associated to the cluster with support $[x_1^-,x_1^+]$ for all M,N sufficiently large. Furthermore, there exists a deterministic ϱ and some small $\epsilon{>}0$, both independent of M, such that $\sup_M x_1^+{+}\epsilon{<}\varrho{<}\inf_M x_2^-{-}\epsilon$.*

The first part of Assumption 3 guarantees that the noise subspace $\boldsymbol{E}_1$ does not vanish in the large dimensional regime when the number of antennas grows to infinity. Hence, the number of sources K is allowed to increase with M but in a way that $\limsup_M K/M<1$. Furthermore, the noise power ($\gamma_1=\sigma^2$) can also vary with the number of antennas, as long as it does not vanish with $M\to\infty$. The second part of the assumption ensures that the eigenvalue cluster associated with the noise eigenvalue γ_1, denoted by $[x_1^-,x_1^+]$ is separated from the clusters of adjacent eigenvalues in the asymptotic eigenvalue distribution of the sample covariance matrix $\hat{\boldsymbol{R}}$. With the aid of this separability assumption, we are now ready to describe the asymptotic behavior of both subspace-based cost functions.

Theorem 1. *Under Assumptions*[1] *1-3 and for each* $\theta\in\Theta$

$$|\hat{\eta}_{\rm c}(\theta)-\bar{\eta}_{\rm c}(\theta)|\to 0 \tag{11}$$

$$|\hat{\eta}_{\rm g}(\theta)-\bar{\eta}_{\rm g}(\theta)|\to 0 \tag{12}$$

almost surely, where $\bar{\eta}_{\rm c}(\theta)$ *and* $\bar{\eta}_{\rm g}(\theta)$ *are two deterministic equivalent objective functions defined as follows. The deterministic equivalent of the MUSIC cost function is defined as*

$$\bar{\eta}_{\rm c}(\theta)=\sum_{m=1}^{\bar{M}}\psi(m)\boldsymbol{a}(\theta)^{\rm H}\boldsymbol{E}_m\boldsymbol{E}_m^{\rm H}\boldsymbol{a}(\theta) \tag{13}$$

with real-valued weights

$$\psi(m)=\begin{cases}1-\frac{1}{K_1}\sum_{r=2}^{\bar{M}}K_r\left(\frac{\gamma_1}{\gamma_r-\gamma_1}-\frac{\mu_1}{\gamma_r-\mu_1}\right), & m=1\\ \frac{\gamma_1}{\gamma_m-\gamma_1}-\frac{\mu_1}{\gamma_m-\mu_1}, & m\neq 1\end{cases}$$

where $\mu_1<\mu_2<\cdots<\mu_{\bar{M}}$ *are the real-valued solutions to the following equation in* μ

$$\frac{1}{N}\sum_{r=1}^{\bar{M}}\frac{K_r\gamma_r}{\gamma_r-\mu}=1. \tag{14}$$

The deterministic equivalent $\bar{\eta}_{\rm g}(\theta)$ *of the g-MUSIC cost function* $\hat{\eta}_{\rm g}(\theta)$ *in* (10) *is defined in* (8).

Proof. See [24, Theorem 2]. A sketch of the proof is provided in Section VI. ■

Remark: The above theorem points out that only the g-MUSIC cost function is an M,N-consistent estimator of the originally intended cost function in (8). However, this does not need to have a direct translation into the consistency of the DoA estimates themselves. It was shown in [15] that for widely spaced sources and a Uniform Linear Array (ULA), both the conventional MUSIC and the g-MUSIC DoA estimators provide M,N-consistent DoA estimates in spite of the inherent inconsistency of the conventional MUSIC cost function. Hence, under certain circumstances, the position of the local minima of the conventional MUSIC cost function converge to the true DoAs, although the global cost function does not. Also, for closely spaced sources, both MUSIC methods provide M,N-consistent DoA estimates. However the g-MUSIC method provides M,N-consistent DoA estimates under lower asymptotic conditions on N, which explains the superiority in DoA estimation accuracy of g-MUSIC over conventional MUSIC in scenarios with closely spaced sources and limited sample size.

In order to analyze the probability of resolution of both MUSIC methods, we next focus on the characterization of the asymptotic fluctuations of both cost functions around the asymptotic deterministic equivalents in Theorem 1.

[1]Gaussianity is not necessary for this result, and can be replaced by a milder condition on the fourth order moments of the observations.

V. Main Result: Asymptotic Fluctuations of the MUSIC and g-MUSIC Cost Function

The objective of this section is to characterize the asymptotic fluctuations of both conventional MUSIC and g-MUSIC cost functions in (9) and (10) around their asymptotic deterministic equivalents. To that effect, we will describe the finite-dimensional asymptotic distribution of these cost functions evaluated at a constant number of L points. Let us therefore consider a fixed set of L directions given by $\bar{\boldsymbol{\theta}}=[\bar{\theta}_1,...,\bar{\theta}_L]^{\rm T}$ within the field of view Θ of the sensor array and denote

$$\hat{\boldsymbol{\eta}}_{\rm c}(\bar{\boldsymbol{\theta}})=[\hat{\eta}_{\rm c}(\bar{\theta}_1),...,\hat{\eta}_{\rm c}(\bar{\theta}_L)]^{\rm T} \tag{15}$$

$$\hat{\boldsymbol{\eta}}_{\rm g}(\bar{\boldsymbol{\theta}})=[\hat{\eta}_{\rm g}(\bar{\theta}_1),...,\hat{\eta}_{\rm g}(\bar{\theta}_L)]^{\rm T}, \tag{16}$$

where $\hat{\eta}_{\rm c}(\theta)$ and $\hat{\eta}_{\rm g}(\theta)$ are given in (9) and (10), respectively. In order to investigate the asymptotic behavior of the two vectors $\hat{\boldsymbol{\eta}}_{\rm c}(\bar{\boldsymbol{\theta}})$ and $\hat{\boldsymbol{\eta}}_{\rm g}(\bar{\boldsymbol{\theta}})$ we will also consider the two L-dimensional vectors $\bar{\boldsymbol{\eta}}_{\rm c}(\bar{\boldsymbol{\theta}})$ and $\bar{\boldsymbol{\eta}}_{\rm g}(\bar{\boldsymbol{\theta}})$ that contain the corresponding deterministic equivalents. These two vectors are respectively defined as (15)-(16) by replacing $\hat{\eta}_{\rm c}(\bar{\theta}_l)$ and $\hat{\eta}_{\rm g}(\bar{\theta}_l)$ with $\bar{\eta}_{\rm c}(\bar{\theta}_l)$ in (13) and $\bar{\eta}_{\rm g}(\bar{\theta}_l)$ in (8), where $l=1,...,L$.

In order to introduce the main result of this section, we need to introduce the asymptotic covariance matrices of the vectors in (15)-(16). Let $\omega(z)$ be defined by inverting the mapping in (7) as follows. When $z\in\mathbb{C}^+\doteq\{z\in\mathbb{C}:{\rm Im}[z]>0\}$, $\omega(z)$ is defined as the unique solution to

$$z=\omega(z)\left(1-\frac{1}{N}\sum_{r=1}^{\bar{M}}\frac{K_r\gamma_r}{\gamma_r-\omega(z)}\right) \tag{17}$$

in $\mathbb{C}^+$. When $z^*\in\mathbb{C}^+$, we take $\omega(z)=\omega^*(z^*)$. Finally, when $z\in\mathbb{R}$, we take $\omega(z)$ to be the unique solution to the above equation such that $\frac{1}{N}\sum_{r=1}^{\bar{M}}\frac{K_r\gamma_r^2}{|\gamma_r-\omega(z)|^2}\leq 1$. It can be shown that $\omega(z)$ is well defined on all $\mathbb{C}$ and holomorphic on $\mathbb{C}\backslash\mathcal{S}$, with derivative

$$\omega'(z)=\frac{\partial\omega(z)}{\partial z}=\left(1-\frac{1}{N}\sum_{r=1}^{\bar{M}}\frac{K_r\gamma_r^2}{(\gamma_r-\omega(z))^2}\right)^{-1}. \tag{18}$$

Using tools from RMT it is shown in Section VI that both the conventional MUSIC and the g-MUSIC cost functions fluctuate around their asymptotic equivalents as Gaussian random vectors. In order to formulate this result, we now define the asymptotic covariance matrices of the corresponding random vectors in (15)-(16) after proper centering and normalization. Regarding the conventional MUSIC algorithm, we define

$$\left[\boldsymbol{\Gamma}_{\rm c}(\bar{\boldsymbol{\theta}})\right]_{p,q}=\sum_{r=1}^{\bar{M}}\sum_{k=1}^{\bar{M}}\Big(\xi_{\rm c}(r,k)\boldsymbol{a}(\bar{\theta}_p)^{\rm H}\boldsymbol{E}_r\boldsymbol{E}_r^{\rm H}\boldsymbol{a}(\bar{\theta}_q) \times\boldsymbol{a}(\bar{\theta}_q)^{\rm H}\boldsymbol{E}_k\boldsymbol{E}_k^{\rm H}\boldsymbol{a}(\bar{\theta}_p)\Big) \tag{19}$$

for $p,q\in\{1,...,L\}$ where the real-valued weights

$$\xi_{\rm c}(r,k)=\begin{cases}\gamma_r\gamma_k\tilde{\xi}_{\rm c}(r,k) & M>N\\ \gamma_r\gamma_k\bar{\xi}_{\rm c}(r,k) & M\leq N\end{cases} \tag{20}$$

differ depending on the number of snapshots N and the number of sensors M. In the undersampled case ($M>N$) the weights are given by $\tilde{\xi}_{\rm c}(r,k)$ in (21) whereas in the oversampled case ($M\leq N$) the weights are given by $\bar{\xi}_{\rm c}(r,k)$ in (22), both at the top of the next page. The real-valued quantities μ_r for $r=1,...,\bar{M}$ are defined as in (14).

Regarding the g-MUSIC cost function, we define

$$\left[\boldsymbol{\Gamma}_{\rm g}(\bar{\boldsymbol{\theta}})\right]_{p,q}=\sum_{r=1}^{\bar{M}}\sum_{k=1}^{\bar{M}}\Big(\xi_{\rm g}(r,k)\boldsymbol{a}(\bar{\theta}_p)^{\rm H}\boldsymbol{E}_r\boldsymbol{E}_r^{\rm H}\boldsymbol{a}(\bar{\theta}_q) \times\boldsymbol{a}(\bar{\theta}_q)^{\rm H}\boldsymbol{E}_k\boldsymbol{E}_k^{\rm H}\boldsymbol{a}(\bar{\theta}_p)\Big) \tag{23}$$

$$\tilde{\xi}_{\rm c}(r,k) = -\frac{N}{K_1}\frac{1}{\left(\frac{1}{N}K_1\gamma_1\right)^2}\left(1-\frac{1}{N}\sum_{m=2}^{\bar{M}}\frac{K_m\gamma_m}{\gamma_m-\gamma_1}\right)^2\delta_{r=k=1} - \frac{1}{\left(\frac{1}{N}K_1\gamma_1\right)^2}\left(1-\frac{1}{N}\sum_{m=2}^{\bar{M}}\frac{K_m\gamma_m^2}{(\gamma_m-\gamma_1)^2}\right)\delta_{r=k=1}$$
$$-\frac{N}{K_1}\frac{1}{(\gamma_k-\gamma_1)^2}\delta_{r=1\neq k} - \frac{N}{K_1}\frac{1}{(\gamma_r-\gamma_1)^2}\delta_{k=1\neq r} + \frac{2}{\pi}\int_{x_1^-}^{x_1^+}\frac{1}{\left|1-\frac{1}{N}\sum_{m=1}^{\bar{M}}\frac{K_m\gamma_m}{\gamma_m-\omega(x)}\right|^2}\frac{\mathrm{Im}[\omega(x)]}{|\gamma_r-\omega(x)|^2|\gamma_k-\omega(x)|^2}\mathrm{d}x \quad (21)$$

$$\bar{\xi}_{\rm c}(r,k) = 2\frac{\mu_1}{\gamma_1}\frac{1}{\left(\frac{1}{N}K_1\gamma_1\right)^2}\left(1-\frac{1}{N}\sum_{m=2}^{\bar{M}}\frac{K_m\gamma_m^2}{(\gamma_m-\gamma_1)(\gamma_m-\mu_1)}\right)\delta_{r=k=1} + 2\frac{\mu_1}{\gamma_1-\mu_1}\frac{1}{\left(\frac{1}{N}K_1\gamma_1\right)^2}\left(1-\frac{1}{N}\sum_{m=2}^{\bar{M}}\frac{K_m\gamma_m}{\gamma_m-\gamma_1}\right)\delta_{r=k=1}$$
$$+2\frac{N}{K_1}\frac{1}{(\gamma_k-\gamma_1)\gamma_1}\frac{\mu_1}{\gamma_k-\mu_1}\delta_{r=1\neq k} + 2\frac{N}{K_1}\frac{1}{(\gamma_r-\gamma_1)\gamma_1}\frac{\mu_1}{\gamma_r-\mu_1}\delta_{k=1\neq r} + \frac{\mu_1^2}{(\gamma_r-\mu_1)^2(\gamma_k-\mu_1)^2}\frac{1}{1-\frac{1}{N}\sum_{m=1}^{\bar{M}}\frac{K_m\gamma_m^2}{(\gamma_m-\mu_1)^2}} + \tilde{\xi}_{\rm c}(r,k) \quad (22)$$

for $p,q\in\{1,...,L\}$ where the real-valued weights $\xi_{\rm g}(r,k)$ are given by

$$\xi_{\rm g}(r,k) = -\frac{N}{K_1}\delta_{r=k=1} + \frac{2}{\pi}\int_{x_1^-}^{x_1^+}\frac{\gamma_r\gamma_k|\omega'(x)|^2\mathrm{Im}[\omega(x)]}{|\gamma_r-\omega(x)|^2|\gamma_k-\omega(x)|^2}\mathrm{d}x. \quad (24)$$

Having introduced these two asymptotic covariance matrices, we next introduce an additional assumption that essentially guarantees that the eigenvalues of the matrices $\mathbf{\Gamma}_{\rm c}(\bar{\boldsymbol{\theta}})$ in (19) and $\mathbf{\Gamma}_{\rm g}(\bar{\boldsymbol{\theta}})$ in (23) are contained in a compact interval of the positive real axis independent of M. This is necessary in order to guarantee that the two random cost functions asymptotically fluctuate around the corresponding deterministic equivalents.

Assumption 4. *Let $\boldsymbol{A}(\bar{\boldsymbol{\theta}})$ denote the $M\times L$ matrix that contains, stacked side by side, the steering vectors $\boldsymbol{a}(\theta)$ evaluated at the directions $\bar{\theta}_1,...,\bar{\theta}_L$. Then, if $\lambda_{\min}(\cdot)$ denotes the minimum eigenvalue of a matrix, we have*

$$\inf_M \sum_{m=2}^{\bar{M}}\lambda_{\min}^2\left(\boldsymbol{A}^{\rm H}(\bar{\boldsymbol{\theta}})\boldsymbol{E}_m\boldsymbol{E}_m^{\rm H}\boldsymbol{A}(\bar{\boldsymbol{\theta}})\right)>0.$$

This assumption is essentially pointing out that the matrix $\boldsymbol{A}(\bar{\boldsymbol{\theta}})$ must be full-rank, and its projection onto the different signal-subspaces $\boldsymbol{E}_2,...,\boldsymbol{E}_{\bar{M}}$ of the true covariance matrix $\boldsymbol{R}$ cannot vanish uniformly. Having introduced this last assumption, we are now in the position to introduce the main result of this paper.

Theorem 2. *Under Assumptions 1-4, we have*

$$\sqrt{N}\mathbf{\Gamma}_{\rm c}(\bar{\boldsymbol{\theta}})^{-1/2}\left(\hat{\boldsymbol{\eta}}_{\rm c}(\bar{\boldsymbol{\theta}})-\bar{\boldsymbol{\eta}}_{\rm c}(\bar{\boldsymbol{\theta}})\right)\xrightarrow{\mathcal{D}}\mathcal{N}(\mathbf{0},\boldsymbol{I}_L) \quad (25)$$

$$\sqrt{N}\mathbf{\Gamma}_{\rm g}(\bar{\boldsymbol{\theta}})^{-1/2}\left(\hat{\boldsymbol{\eta}}_{\rm g}(\bar{\boldsymbol{\theta}})-\bar{\boldsymbol{\eta}}_{\rm g}(\bar{\boldsymbol{\theta}})\right)\xrightarrow{\mathcal{D}}\mathcal{N}(\mathbf{0},\boldsymbol{I}_L) \quad (26)$$

where $\xrightarrow{\mathcal{D}}$ denotes convergence in distribution and where $\mathbf{\Gamma}_{\rm c}(\bar{\boldsymbol{\theta}})\in\mathbb{R}^{L\times L}$ is given in (19) *and $\mathbf{\Gamma}_{\rm g}(\bar{\boldsymbol{\theta}})\in\mathbb{R}^{L\times L}$ is given in* (23)*, respectively.*

Proof. The proof is given in Section VI. ∎

Remark: The order of convergence in (25) and (26) is $\mathcal{O}(N^{-1/2})$. The real-valued integrals in (20) and (24) can be computed using numerical integration techniques such as the Riemann sum or the Simpson's rule.

A. Probability of Resolution

The practical relevance of a DoA estimator highly depends on its computational complexity as well as its estimation accuracy. For the estimation accuracy of subspace-based DoA estimators like MUSIC and g-MUSIC the so called threshold effect is of major interest. The threshold effect describes an abrupt increase in the Mean Square Error (MSE) below a certain SNR threshold and can be characterized by analyzing the resolution capabilities of the underlying DoA estimator [2], [7], [28]. In the literature, several criteria to declare resolution between two neighboring sources have been introduced [29]–[32]. In case of a one-dimensional spectral search based DoA estimator, one may declare that two sources located at DoAs $\boldsymbol{\theta}=[\theta_1,\theta_2]^{\rm T}$ are resolved if both DoA estimation errors, namely $|\theta_1-\hat{\theta}_1|$ and $|\theta_2-\hat{\theta}_2|$ are smaller than $|\theta_1-\theta_2|/2$ [31]. A popular alternative is to evaluate the cost function at both true DoAs and to verify if the cost at the mid-angle $(\theta_1+\theta_2)/2$ is larger than at the true DoAs [32]. Hence, under the latter criterion resolution is declared if $\boldsymbol{u}^{\rm T}\hat{\boldsymbol{\eta}}(\bar{\boldsymbol{\theta}})<0$ where

$$\boldsymbol{u}=\begin{bmatrix}1/2\\1/2\\-1\end{bmatrix},\quad \bar{\boldsymbol{\theta}}=\begin{bmatrix}\theta_1\\\theta_2\\\frac{\theta_1+\theta_2}{2}\end{bmatrix},\quad \hat{\boldsymbol{\eta}}(\bar{\boldsymbol{\theta}})=\begin{bmatrix}\hat{\eta}(\theta_1)\\\hat{\eta}(\theta_2)\\\hat{\eta}\left(\frac{\theta_1+\theta_2}{2}\right)\end{bmatrix}$$

and $\hat{\eta}(\theta)$ denotes a generic cost function. Using the previously derived asymptotic stochastic behavior of the cost function vector $\hat{\boldsymbol{\eta}}(\bar{\boldsymbol{\theta}})$ in Theorem 2, the probability of resolution can be expressed as the cumulative distribution function [33]

$$P_{\rm res}=\Pr\left(\boldsymbol{u}^{\rm T}\hat{\boldsymbol{\eta}}(\bar{\boldsymbol{\theta}})<0\right)=\int_{-\infty}^{0}f_{\boldsymbol{u}^{\rm T}\hat{\boldsymbol{\eta}}(\bar{\boldsymbol{\theta}})}(x)\mathrm{d}x \quad (27)$$

where $f_{\boldsymbol{u}^{\rm T}\hat{\boldsymbol{\eta}}(\bar{\boldsymbol{\theta}})}(x)$ denotes the pdf of the test quantity $\boldsymbol{u}^{\rm T}\hat{\boldsymbol{\eta}}(\bar{\boldsymbol{\theta}})$ that can be asymptotically approximated by a Gaussian distribution with law $\mathcal{N}(\boldsymbol{u}^{\rm T}\bar{\boldsymbol{\eta}}(\bar{\boldsymbol{\theta}}),N^{-1}\boldsymbol{u}^{\rm T}\mathbf{\Gamma}(\bar{\boldsymbol{\theta}})\boldsymbol{u})$, where $\bar{\boldsymbol{\eta}}(\bar{\boldsymbol{\theta}})$ and $\mathbf{\Gamma}(\bar{\boldsymbol{\theta}})$ take the form in (13)-(19) or in (8)-(23) depending on the subspace method under evaluation [34].

VI. Proof of Theorem 2

We begin by reviewing some standard arguments that allow to represent the MUSIC and g-MUSIC cost functions as contour integrals of the resolvent of the sample covariance matrix, which is a matrix-valued function of a complex variable $z\in\mathbb{C}\backslash\mathbb{R}$ defined as $\hat{\boldsymbol{Q}}(z)=(\hat{\boldsymbol{R}}-z\boldsymbol{I}_M)^{-1}$ [24], [25]. Observe that, using the eigenvalue decomposition of $\hat{\boldsymbol{R}}$ in (5) we are able to write

$$\hat{\boldsymbol{Q}}(z)=\sum_{m=1}^{M}\frac{1}{\hat{\lambda}_m-z}\hat{\boldsymbol{e}}_m\hat{\boldsymbol{e}}_m^{\rm H}$$

and therefore a direct application of the Cauchy integral theorem shows that

$$\sum_{m=1}^{M}\hat{\boldsymbol{e}}_m\hat{\boldsymbol{e}}_m^{\rm H}=\frac{1}{2\pi\mathrm{j}}\oint_{\mathcal{C}_z}\hat{\boldsymbol{Q}}(z)\mathrm{d}z \quad (28)$$

where $\mathcal{C}_z$ is a clockwise oriented simple closed contour that encloses only the $K_1{=}M{-}K$ smallest eigenvalues of the sample covariance matrix $\hat{\boldsymbol{R}}$.

Now, it is well known that for all M,N sufficiently large, the $M-K$ smallest eigenvalues of $\hat{\boldsymbol{R}}$ are located inside $[x_1,x_1^+]$ plus $\{0\}$ if $M>N$ [26], [35]. Thanks to this fact, we can always deform the contour in (28) and make it independent of M. This deterministic contour may cross the real axis at the points ϱ

(defined in Assumption 3) and any other point in the negative real axis. Consequently, one can investigate the asymptotic behavior of the eigenvectors of the sample covariance matrix by equivalently characterizing the asymptotic behavior of the resolvent $\hat{\boldsymbol{Q}}(z)$.

A. Asymptotic Equivalent of MUSIC and Derivation of g-MUSIC

Under Assumptions 1-2 and for fixed θ and $z\in\mathbb{C}\backslash\mathbb{R}$ we have

$$\left|\boldsymbol{a}^{\mathrm{H}}(\theta)\hat{\boldsymbol{Q}}(z)\boldsymbol{a}(\theta)-\frac{\omega(z)}{z}\boldsymbol{a}^{\mathrm{H}}(\theta)(\boldsymbol{R}-\omega(z)\boldsymbol{I}_M)^{-1}\boldsymbol{a}(\theta)\right|\to 0 \quad (29)$$

almost surely [22], [23], where $\omega(z)$ is defined as in (17). A direct application of the dominated convergence theorem therefore shows that, since

$$\hat{\eta}_{\mathrm{c}}(\theta)=\frac{1}{2\pi \mathrm{j}}\oint_{\mathcal{C}_z}\boldsymbol{a}^{\mathrm{H}}(\theta)\hat{\boldsymbol{Q}}(z)\boldsymbol{a}(\theta)\mathrm{d}z$$

we can write

$$\left|\hat{\eta}_{\mathrm{c}}(\theta)-\frac{1}{2\pi \mathrm{j}}\oint_{\mathcal{C}_z}\frac{\omega(z)}{z}\boldsymbol{a}^{\mathrm{H}}(\theta)(\boldsymbol{R}-\omega(z)\boldsymbol{I}_M)^{-1}\boldsymbol{a}(\theta)\mathrm{d}z\right|\to 0.$$

The right hand side of the above difference can be shown to coincide with the expression in (13) after applying the change of variables $z=z(\omega)$ as given in (7) and solving the corresponding integral via Cauchy integration [24].

A very similar idea can be used to derive the g-MUSIC cost function. We begin by expressing the cost function that we want to estimate using again the Cauchy integral, that is

$$\bar{\eta}_{\mathrm{g}}(\theta)=\frac{1}{2\pi \mathrm{j}}\oint_{\mathcal{C}_\omega}\boldsymbol{a}^{\mathrm{H}}(\theta)(\boldsymbol{R}-\omega\boldsymbol{I}_M)^{-1}\boldsymbol{a}(\theta)\mathrm{d}\omega$$

where now $\mathcal{C}_\omega$ is a clockwise oriented simple closed contour that encloses γ_1 and no other eigenvalue. In particular, it can be shown that [6] $z\mapsto\omega(z)$ in (17) can be used as parametrization of such a contour, in the sense that we can choose $\mathcal{C}_\omega=\omega(\mathcal{C}_z)$ with $\mathcal{C}_z$ as defined above. It can be seen that the generated contour has the properties that we are looking for [6], and consequently we can express

$$\bar{\eta}_{\mathrm{g}}(\theta)=\frac{1}{2\pi \mathrm{j}}\oint_{\mathcal{C}_z}\boldsymbol{a}^{\mathrm{H}}(\theta)(\boldsymbol{R}-\omega(z)\boldsymbol{I}_M)^{-1}\boldsymbol{a}(\theta)\omega'(z)\mathrm{d}z \quad (30)$$

with $\omega'(z)$ as in (18). Now, observe that the above contour does not depend on M, so that invoking again the dominated convergence theorem we can find an M,N-consistent estimator of $\bar{\eta}_{\mathrm{g}}(\theta)$ by simply replacing the integrand above with a corresponding M,N-consistent estimate. Using (29) we readily see that we only need to find an M,N-consistent estimator of $\omega(z)$ and $\omega'(z)$. An M,N-consistent estimator of $\omega(z)$ can be obtained by using the well-known fact that [22], [23], under Assumptions 1-2 we have

$$\left|\frac{1}{M}\mathrm{tr}\left[\hat{\boldsymbol{Q}}(z)\right]-\frac{\omega(z)}{z}\frac{1}{M}\mathrm{tr}\left[(\boldsymbol{R}-\omega(z)\boldsymbol{I}_M)^{-1}\right]\right|\to 0$$

almost surely for fixed $z\in\mathbb{C}\backslash\mathbb{R}$. Using the fact that $\omega(z)$ is a solution to the equation in (17), this can be reformulated as

$$\left|\omega(z)-z\left(1-\frac{1}{N}\mathrm{tr}\left[\hat{\boldsymbol{R}}(\hat{\boldsymbol{R}}-z\boldsymbol{I}_M)^{-1}\right]\right)^{-1}\right|\to 0$$

(see [19, Lemma 8]). Therefore, the right hand side of the above difference, which will be denoted as $\hat{\omega}(z)$, is an M,N-consistent estimator of $\omega(z)$. Furthermore, the M,N-consistent estimator of $\omega'(z)$ can be obtained by using the fact that convergence of holomorphic functions imply the convergence of their derivatives, so that

$$\hat{\omega}'(z)=\frac{\partial\hat{\omega}(z)}{\partial z}=\frac{\hat{\omega}(z)}{z}+\frac{\hat{\omega}(z)^2}{z}\frac{1}{N}\mathrm{tr}\left[\hat{\boldsymbol{R}}\left(\hat{\boldsymbol{R}}-z\boldsymbol{I}_M\right)^{-2}\right]$$

is an M,N-consistent estimator of $\omega'(z)$. We can therefore obtain the M,N-consistent estimator of the g-MUSIC cost function by inserting these estimators into the Cauchy integral in (30), that is

$$\hat{\eta}_{\mathrm{g}}(\theta)=\frac{1}{2\pi \mathrm{j}}\oint_{\mathcal{C}_z}\boldsymbol{a}^{\mathrm{H}}(\theta)\hat{\boldsymbol{Q}}(z)\boldsymbol{a}(\theta)\frac{z}{\hat{\omega}(z)}\hat{\omega}'(z)\mathrm{d}z. \quad (31)$$

The contour integral in (31) is solved in closed-form in [6, Theorem 2] (also see [25, Theorem 3]) using conventional residue calculus, which yields the expression in (10).

B. Asymptotic Fluctuations

Let us now consider again the fluctuations of these two cost functions at a set of L fixed distinct angles, $\bar{\theta}_1,\ldots,\bar{\theta}_L$. Using the previously derived asymptotic equivalents of the MUSIC cost function we can express

$$\sqrt{N}\big(\hat{\eta}_{\mathrm{c}}(\bar{\theta}_l)-\bar{\eta}_{\mathrm{c}}(\bar{\theta}_l)\big)=\frac{1}{2\pi \mathrm{j}}\oint_{\mathcal{C}_z}\sqrt{N}\boldsymbol{a}^{\mathrm{H}}(\bar{\theta}_l)\left(\hat{\boldsymbol{Q}}(z)-\bar{\boldsymbol{Q}}(z)\right)\boldsymbol{a}(\bar{\theta}_l)\mathrm{d}z$$

where we have introduced $\bar{\boldsymbol{Q}}(z)=\frac{\omega(z)}{z}(\boldsymbol{R}-\omega(z)\boldsymbol{I}_M)^{-1}$. Similarly, for the g-MUSIC cost function we have

$$\sqrt{N}\big(\hat{\eta}_{\mathrm{g}}(\bar{\theta}_l)-\bar{\eta}_{\mathrm{g}}(\bar{\theta}_l)\big)$$
$$=\frac{1}{2\pi \mathrm{j}}\oint_{\mathcal{C}_z}\sqrt{N}\boldsymbol{a}^{\mathrm{H}}(\bar{\theta}_l)\left(\frac{z\hat{\omega}'(z)}{\hat{\omega}(z)}\hat{\boldsymbol{Q}}(z)-\frac{z\omega'(z)}{\omega(z)}\bar{\boldsymbol{Q}}(z)\right)\boldsymbol{a}(\bar{\theta}_l)\mathrm{d}z.$$

It can be seen that both expressions take the form

$$\sqrt{N}\big(\hat{\eta}(\bar{\theta}_l)-\bar{\eta}(\bar{\theta}_l)\big)$$
$$=\frac{1}{2\pi \mathrm{j}}\oint_{\mathcal{C}_z}\sqrt{N}\boldsymbol{a}^{\mathrm{H}}(\bar{\theta}_l)\left(\hat{h}(z)\hat{\boldsymbol{Q}}(z)-\bar{h}(z)\bar{\boldsymbol{Q}}(z)\right)\boldsymbol{a}(\bar{\theta}_l)\mathrm{d}z \quad (32)$$

where $\hat{\eta}(\theta)$ is a generic cost function with deterministic equivalent $\bar{\eta}(\theta)$. In case of the conventional MUSIC cost function we have $\hat{h}(z)=1$ and $\bar{h}(z)=1$ whereas in case of the g-MUSIC cost function $\hat{h}(z)=\frac{z\hat{\omega}'(z)}{\hat{\omega}(z)}$ and $\bar{h}(z)=\frac{z\omega'(z)}{\omega(z)}$. It is well known [36], [37] that the statistic in (32) asymptotically fluctuates as a Gaussian random variable with zero-mean and positive variance. However, we are interested in the more general case of the asymptotic joint distribution of a collection of random variables, namely

$$\sqrt{N}\big(\hat{\boldsymbol{\eta}}(\bar{\boldsymbol{\theta}})-\bar{\boldsymbol{\eta}}(\bar{\boldsymbol{\theta}})\big)=\begin{bmatrix}\sqrt{N}(\hat{\eta}(\bar{\theta}_1)-\bar{\eta}(\bar{\theta}_1))\\ \vdots\\ \sqrt{N}(\hat{\eta}(\bar{\theta}_L)-\bar{\eta}(\bar{\theta}_L))\end{bmatrix} \quad (33)$$

where $\sqrt{N}(\hat{\eta}(\bar{\theta}_l)-\bar{\eta}(\bar{\theta}_l)$ for $l=1,\ldots,L$ is defined in (32). The second order asymptotic behavior in Theorem 2 is derived by establishing pointwise convergence of the characteristic function of the statistic $\sqrt{N}\big(\hat{\boldsymbol{\eta}}(\bar{\boldsymbol{\theta}})-\bar{\boldsymbol{\eta}}(\bar{\boldsymbol{\theta}})\big)$ in (33) to the characteristic function of a Gaussian distributed random variable. Moreover, by the Cramér-Wold device [38] it is sufficient to establish that the one-dimensional projection of the statistic in (33), namely

$$\sum_{l=1}^{L}\sqrt{N}w_l\big(\hat{\eta}(\bar{\theta}_l)-\bar{\eta}(\bar{\theta}_l)\big)=\sqrt{N}\boldsymbol{w}^{\mathrm{T}}\big(\hat{\boldsymbol{\eta}}(\bar{\boldsymbol{\theta}})-\bar{\boldsymbol{\eta}}(\bar{\boldsymbol{\theta}})\big) \quad (34)$$

is asymptotically Gaussian distributed for any collection of real-valued bounded quantities $\boldsymbol{w}=[w_1,\ldots,w_L]^{\mathrm{T}}\in\mathbb{R}^L$ to show that (33) is asymptotically jointly Gaussian distributed. Additionally, by Lévy's continuity Theorem convergence in distribution of a set of random variables can be proven by establishing pointwise convergence of the characteristic functions. Let $\chi(r)$ be defined as $\chi(r)=\exp\left(\mathrm{j}r\sqrt{N}\boldsymbol{w}^{\mathrm{T}}\big(\hat{\boldsymbol{\eta}}(\bar{\boldsymbol{\theta}})-\bar{\boldsymbol{\eta}}(\bar{\boldsymbol{\theta}})\big)\right)$ and let $\mathbb{E}[\chi(r)]$ be the corresponding characteristic function of the one-dimensional projection in (34). The target is to study the asymptotic behavior of the characteristic function $\mathbb{E}[\chi(r)]$ in the asymptotic regime where $M,N\to\infty$ at the same rate by establishing convergence towards the characteristic function of a Gaussian random variable with zero-mean and covariance $\boldsymbol{w}^{\mathrm{T}}\boldsymbol{\Gamma}(\bar{\boldsymbol{\theta}})\boldsymbol{w}$, that is $\mathbb{E}[\chi(r)]-\bar{\chi}(r)\to 0$ where

$$\bar{\chi}(r)=\exp\left(-r^2\frac{\boldsymbol{w}^{\mathrm{T}}\boldsymbol{\Gamma}(\bar{\boldsymbol{\theta}})\boldsymbol{w}}{2}\right). \tag{35}$$

In (35), $\boldsymbol{\Gamma}(\bar{\boldsymbol{\theta}})\in\mathbb{R}^{L\times L}$ characterizes the second order asymptotic behavior of the statistic $\sqrt{N}(\hat{\boldsymbol{\eta}}(\bar{\boldsymbol{\theta}})-\bar{\boldsymbol{\eta}}(\bar{\boldsymbol{\theta}}))$ in (33), which is the quantity of interest. In the asymptotic analysis of the characteristic function $\mathbb{E}[\chi(r)]$ of the one-dimensional projection $\sqrt{N}\boldsymbol{w}^{\mathrm{T}}(\hat{\boldsymbol{\eta}}(\bar{\boldsymbol{\theta}})-\bar{\boldsymbol{\eta}}(\bar{\boldsymbol{\theta}}))$ we rely on the integration by parts formula [39]–[41] and the Nash-Poincaré inequality [40]–[42]. It can be shown that the second order asymptotic behavior of the statistic in (34) is computed as follows.

Theorem 3. *Consider an $L\times L$ matrix $\boldsymbol{\Gamma}(\bar{\boldsymbol{\theta}})$ the elements of which are given by*

$$\left[\boldsymbol{\Gamma}(\bar{\boldsymbol{\theta}})\right]_{p,q}=\frac{1}{2\pi\mathrm{j}}\frac{1}{2\pi\mathrm{j}}\oint_{\mathcal{C}_{\omega_1}}\oint_{\mathcal{C}_{\omega_2}}\bar{h}(z(\omega_1))\bar{h}(z(\omega_2))\frac{\partial z(\omega_1)}{\partial\omega_1}\frac{\partial z(\omega_2)}{\partial\omega_2}\times\frac{\omega_1}{z(\omega_1)}\frac{\omega_2}{z(\omega_2)}\frac{\Upsilon_{p,q}(\omega_1,\omega_2)}{1-\Omega(\omega_1,\omega_2)}\mathrm{d}\omega_2\mathrm{d}\omega_1 \tag{36}$$

for $p,q\in\{1,\ldots,L\}$, where $\mathcal{C}_{\omega_1}$, $\mathcal{C}_{\omega_2}$ are two clockwise oriented simple closed contours enclosing only the smallest eigenvalue γ_1 of $\boldsymbol{R}$,

$$\begin{aligned}\Upsilon_{p,q}(\omega_1,\omega_2)=&\boldsymbol{a}(\bar{\theta}_p)^{\mathrm{H}}(\boldsymbol{R}-\omega_1\boldsymbol{I}_M)^{-1}\boldsymbol{R}(\boldsymbol{R}-\omega_2\boldsymbol{I}_M)^{-1}\boldsymbol{a}(\bar{\theta}_q)\\&\times\boldsymbol{a}(\bar{\theta}_q)^{\mathrm{H}}(\boldsymbol{R}-\omega_2\boldsymbol{I}_M)^{-1}\boldsymbol{R}(\boldsymbol{R}-\omega_1\boldsymbol{I}_M)^{-1}\boldsymbol{a}(\bar{\theta}_p)\end{aligned} \tag{37}$$

and where

$$\Omega(\omega_1,\omega_2)=\frac{1}{N}\mathrm{tr}\left[\boldsymbol{R}(\boldsymbol{R}-\omega_1\boldsymbol{I}_M)^{-1}\boldsymbol{R}(\boldsymbol{R}-\omega_2\boldsymbol{I}_M)^{-1}\right]. \tag{38}$$

Function $z(\omega)$ is defined in (7) and its first order derivative can be computed as

$$\frac{\partial z(\omega)}{\partial\omega}=1-\frac{1}{N}\sum_{r=1}^{\bar{M}}\frac{K_r\gamma_r^2}{(\gamma_r-\omega)^2}. \tag{39}$$

Let Assumptions 1-3 hold true and assume additionally that the eigenvalues of $\boldsymbol{\Gamma}(\bar{\boldsymbol{\theta}})$ are all located in a compact interval of the positive real axis independent of M. Then, $\sqrt{N}\boldsymbol{\Gamma}(\bar{\boldsymbol{\theta}})^{-1/2}(\hat{\boldsymbol{\eta}}(\bar{\boldsymbol{\theta}})-\bar{\boldsymbol{\eta}}(\bar{\boldsymbol{\theta}}))$ in (33) converges in law to a standardized multivariate Gaussian distribution.

Proof. A detailed proof is provided in [43]. ■

With the help of Theorem 3 above, the proof of Theorem 2 follows directly once we have been able to (i) compute the integral that defines the asymptotic covariance matrix for these two cost functions and (ii) prove that the maximum (resp. minimum) eigenvalue of these two covariance matrices is bounded (resp. bounded away from zero).

Let us first consider the computation of the two asymptotic covariance matrices, which follows from solving the integral in (36) for $\bar{h}(z(\omega))=1$ (conventional MUSIC) and for $\bar{h}(z(\omega))=\frac{z(\omega)}{\omega}\frac{\partial\omega(z)}{\partial z}$ (g-MUSIC). To simplify the computation of the asymptotic covariance, we express $\boldsymbol{\Gamma}(\bar{\boldsymbol{\theta}})$ in (36) as

$$\boldsymbol{\Gamma}(\bar{\boldsymbol{\theta}})=\sum_{r=1}^{\bar{M}}\sum_{k=1}^{\bar{M}}\xi(r,k)\boldsymbol{A}^{\mathrm{H}}(\bar{\boldsymbol{\theta}})\boldsymbol{E}_r\boldsymbol{E}_r^{\mathrm{H}}\boldsymbol{A}(\bar{\boldsymbol{\theta}})\odot\left(\boldsymbol{A}^{\mathrm{H}}(\bar{\boldsymbol{\theta}})\boldsymbol{E}_k\boldsymbol{E}_k^{\mathrm{H}}\boldsymbol{A}(\bar{\boldsymbol{\theta}})\right)^{\mathrm{T}} \tag{40}$$

where $\odot$ denotes element-wise product and where the coefficients $\xi(r,k)$ are defined as

$$\xi(r,k)=\frac{1}{2\pi\mathrm{j}}\oint_{\mathcal{C}_{\omega_1}}\bar{h}(z(\omega_1))\frac{\omega_1}{z(\omega_1)}\frac{\partial z(\omega_1)}{\partial\omega_1}\frac{\gamma_r\gamma_k\mathcal{I}_{r,k}(\omega_1)}{(\gamma_r-\omega_1)(\gamma_k-\omega_1)}\mathrm{d}\omega_1, \tag{41}$$

with

$$\mathcal{I}_{r,k}(\omega_1)=\frac{1}{2\pi\mathrm{j}}\oint_{\mathcal{C}_{\omega_2}}\bar{h}(z(\omega_2))\frac{\omega_2}{z(\omega_2)}\frac{\partial z(\omega_2)}{\partial\omega_2}\frac{\frac{1}{(\gamma_r-\omega_2)(\gamma_k-\omega_2)}}{1-\Omega(\omega_1,\omega_2)}\mathrm{d}\omega_2. \tag{42}$$

These two integrals are solved in Appendices A and B for the conventional MUSIC and the g-MUSIC cost functions, leading to the expressions in (19) and (23) respectively.

To obtain an upper bound on the spectral norm of $\boldsymbol{\Gamma}(\bar{\boldsymbol{\theta}})$, we consider the expression in (40) and observe that the coefficients $\xi(r,k)$ are all real-valued and positive. The fact that they are real-valued follows from the property $z(\omega^*)=z^*(\omega)$ in (7) as well as the fact that $\bar{h}(z^*)=\bar{h}^*(z)$ for both definitions of this function. The fact that the coefficients $\xi(r,k)$ in (41) are non-negative can be shown by using the following results.

Lemma 1. *Let $\Omega(\omega_1,\omega_2)$ be defined as in (38). Then,*

$$\sup_M\sup_{(z_1,z_2)\in\mathcal{C}_z\times\mathcal{C}_z}|\Omega(\omega(z_1),\omega(z_2))|<1. \tag{43}$$

Proof. By the Cauchy-Schwarz inequality, we have $|\Omega(\omega(z_1),\omega(z_2))|^2\leq\tilde{\Psi}(\omega(z_1))\tilde{\Psi}(\omega(z_1))$ with

$$\tilde{\Psi}(\omega)=\frac{1}{N}\sum_{m=1}^{\bar{M}}K_m\frac{\gamma_m^2}{|\gamma_m-\omega|^2}. \tag{44}$$

Hence, it is sufficient to prove that $\sup_M\sup_{z\in\mathcal{C}_z}|\tilde{\Psi}(\omega(z))|<1$. Let us first consider $z\in\mathbb{C}^+$. Taking imaginary parts on both sides of (17) we see that

$$\tilde{\Psi}(\omega(z))=1-\frac{\mathrm{Im}[z]}{\mathrm{Im}[\omega(z)]}$$

where we recall that $\mathrm{Im}[\omega(z)]>0$ when $\mathrm{Im}[z]>0$. This implies that $\sup_M\tilde{\Psi}(\omega(z))\leq 1$ and $\inf_M\mathrm{Im}[\omega(z)]>0$. In order to see that the inequality $\sup_M\tilde{\Psi}(\omega(z))\leq 1$ must be strict, we reason by contradiction. Assume that the equality holds, and consider a subsequence M' such that $\tilde{\Psi}(\omega(z))\to 1$, implying $\mathrm{Im}[\omega(z)]\to\infty$, as $M'\to\infty$. Now, using the fact that $|\gamma_m-\omega(z)|^2\geq\mathrm{Im}[w(z)]^2$ we see from the definition of $\tilde{\Psi}(\omega(z))$ in (44) that $\tilde{\Psi}(\omega(z))\leq\mathrm{Im}[\omega(z)]^{-2}\frac{1}{N}\sum_{m=1}^{\bar{M}}K_m\gamma_m^2\to 0$ along that subsequence, leading to contradiction.

Consider now $z\in\mathcal{C}_z\cap\mathbb{R}$ and observe that this means that either $z<0$ or $z=\varrho$ in Assumption 3, which are the two crossing points of the contour on the real axis. Assume first that $z=\varrho$ and consider ω_1^+ as right hand side of the first cluster of the support $\mathcal{S}$ and ω_2^- as the left hand side of the second cluster such that $\gamma_1<\omega_1^+<\omega(\varrho)<\omega_2^-<\gamma_2$ (the case $z<0$ follows by similar arguments). It can be observed that $\tilde{\Psi}(\omega)$ in (44) is a strongly convex function since the second order derivative w.r.t. ω

$$\tilde{\Psi}''(\omega)=\frac{6}{N}\sum_{r=1}^{\bar{M}}\frac{K_r\gamma_r^2}{(\gamma_r-\omega)^4} \tag{45}$$

is lower bounded by a positive quantity q, namely

$$q=\inf_M\inf_{\omega\in(\omega_1^+,\omega_2^-)}\tilde{\Psi}''(\omega)>\frac{3}{4}\frac{1}{N}\sum_{r=1}^{\bar{M}}\frac{K_r\gamma_r^2}{\gamma_r^4+\gamma_2^4}>0.$$

By strong convexity it follows that

$$\begin{aligned}\tilde{\Psi}(\omega_2^-)-\tilde{\Psi}(\omega(\varrho))&\geq\tilde{\Psi}'(\omega(\varrho))(\omega_2^--\omega(\varrho))+\frac{q}{2}(\omega_2^--\omega(\varrho))^2\\\tilde{\Psi}(\omega_1^+)-\tilde{\Psi}(\omega(\varrho))&\geq-\tilde{\Psi}'(\omega(\varrho))(\omega(\varrho)-\omega_1^+)+\frac{q}{2}(\omega_1^+-\omega(\varrho))^2.\end{aligned}$$

Using the fact that $\tilde{\Psi}(\omega_2^-)=1$ and $\tilde{\Psi}(\omega_1^+)=1$ we obtain

$$1-\tilde{\Psi}(\omega(\varrho))\geq\begin{cases}\tilde{\Psi}'(\omega(\varrho))(\omega_2^- -\omega(\varrho))+\frac{q}{2}(\omega_2^- -\omega(\varrho))^2\\ -\tilde{\Psi}'(\omega(\varrho))(\omega(\varrho)-\omega_1^+)+\frac{q}{2}(\omega_1^+ -\omega(\varrho))^2.\end{cases}$$

Hence, $\inf_M 1-\tilde{\Psi}(\omega(\varrho))>\frac{q}{2}\min\left[(\omega_2^- -\omega(\varrho))^2,(\omega_1^+ -\omega(\varrho))^2\right]>0$ and therefore $\sup_M\tilde{\Psi}(\omega(\varrho))<1$. The boundedness of $\tilde{\Psi}(\omega(z))$ at the second crossing point with the real axis $z<0$ follows by similar reasoning. ■

The fact that $\Omega(\omega_1,\omega_2)$ is uniformly bounded on $\mathcal{C}_\omega\times\mathcal{C}_\omega$ implies that we can take a power series expansion of the term $(1-\Omega(\omega_1,\omega_2))^{-1}$ and write

$$\xi(r,k)=\gamma_r\gamma_k\sum_{n\geq 0}\frac{1}{N^n}\sum_{r_1+\ldots+r_{\bar{M}}=n}\binom{n}{r_1,\ldots,r_{\bar{M}}}\prod_{m=1}^{\bar{M}}K_m^{r_m}\gamma_m^{2r_m}\times\left(\frac{1}{2\pi\mathrm{j}}\oint_{\mathcal{C}_z}\frac{\omega(z)}{z}\frac{\bar{h}(z)}{(\gamma_r-\omega(z))(\gamma_k-\omega(z))}\prod_{m=1}^{\bar{M}}\frac{1}{(\gamma_m-\omega(z))^{r_m}}\mathrm{d}z\right)^2 \tag{46}$$

where we employed the multinomial theorem to factor out the different powers $\Omega^n(\omega_1,\omega_2)$, $n\geq 0$. An immediate consequence of the above decomposition is the fact that the coefficients $\xi(r,k)$ are non-negative. This will be useful in order to determine the appropriate lower bound on the corresponding covariance matrix.

Lemma 2. *Under Assumptions 1-3, we have* $\sup_M\|\boldsymbol{\Gamma}_{\mathrm{c}}(\bar{\boldsymbol{\theta}})\|<+\infty$ *and* $\sup_M\|\boldsymbol{\Gamma}_{\mathrm{g}}(\bar{\boldsymbol{\theta}})\|<+\infty$.

Proof. Consider the general expression in (40) and assume that we are able to find a positive constant κ such that $\sup_M\sup_{r,k}\xi(r,k)<\kappa$. It will immediately follow that

$$\|\boldsymbol{\Gamma}(\bar{\boldsymbol{\theta}})\|\leq\kappa\left\|\sum_{r=1}^{\bar{M}}\sum_{k=1}^{\bar{M}}\boldsymbol{A}^{\mathrm{H}}(\bar{\boldsymbol{\theta}})\boldsymbol{E}_r\boldsymbol{E}_r^{\mathrm{H}}\boldsymbol{A}(\bar{\boldsymbol{\theta}})\odot\left(\boldsymbol{A}^{\mathrm{H}}(\bar{\boldsymbol{\theta}})\boldsymbol{E}_k\boldsymbol{E}_k^{\mathrm{H}}\boldsymbol{A}(\bar{\boldsymbol{\theta}})\right)^{\mathrm{T}}\right\|=\kappa\left\|\boldsymbol{A}^{\mathrm{H}}(\bar{\boldsymbol{\theta}})\boldsymbol{A}(\bar{\boldsymbol{\theta}})\odot\left(\boldsymbol{A}^{\mathrm{H}}(\bar{\boldsymbol{\theta}})\boldsymbol{A}(\bar{\boldsymbol{\theta}})\right)^{\mathrm{T}}\right\|\leq L\kappa$$

where in the last inequality we have used the fact that the steering vectors have unit norm and the spectral norm of a matrix is upper bounded by its trace. Hence, we only need to find an upper bound on the coefficients. Following the definition of these coefficients in (46) we can readily see that

$$\xi(r,k)\leq\frac{\gamma_r\gamma_k}{1-\bar{\Omega}}\left(\frac{1}{2\pi\mathrm{j}}\oint_{\mathcal{C}_z}|\bar{h}(z)|\frac{|\omega(z)|}{|z|}\frac{1}{|\gamma_r-\omega(z)||\gamma_k-\omega(z)|}|\mathrm{d}z|\right)^2 \tag{47}$$

where $\bar{\Omega}=\sup_{M,(\omega_1,\omega_2)\in\mathcal{C}_\omega\times\mathcal{C}_\omega}\Omega(\omega_1,\omega_2)<1$. Now, from the proof of Lemma 1 it directly follows that $\inf_{M,\omega\in\mathcal{C}_\omega}|\omega(z)-\gamma_k|>0$ for $k=1,\ldots,\bar{M}$. On the other hand, taking real and imaginary part on both sides of (17) it can be shown by contradiction that for bounded $|z|<\infty$ we have $\sup_M|\omega(z)/z|<\infty$.

This directly shows that the coefficients $\xi(r,k)$ are bounded for the MUSIC cost function, which has $\bar{h}(z)=1$. In order to prove boundedness of the g-MUSIC covariance $\boldsymbol{\Gamma}_{\mathrm{g}}(\bar{\boldsymbol{\theta}})$ we only need to show that $\sup_M|\omega'(z)|<\infty$ since $\bar{h}(z)=\frac{z}{\omega(z)}\omega'(z)$ and $\frac{z}{\omega(z)}$ cancels out with $\frac{\omega(z)}{z}$ in (47). The upper bound $\sup_M|\omega'(z)|<\infty$ follows from the fact that, by the triangular inequality, $\sup_M|\omega'(z)|\leq\sup_M(1-|\tilde{\Psi}(\omega(z))|)^{-1}<1$. This completes the proof of Lemma 2. ■

We finally conclude the proof of Theorem 2 by showing that the smallest eigenvalue of the two asymptotic covariance matrices is bounded away from zero.

Lemma 3. *Under Assumptions 1-4, we have* $\inf_M\lambda_{\min}(\boldsymbol{\Gamma}_{\mathrm{c}}(\bar{\boldsymbol{\theta}}))>0$ *and* $\inf_M\lambda_{\min}(\boldsymbol{\Gamma}_{\mathrm{g}}(\bar{\boldsymbol{\theta}}))>0$, *where* $\lambda_{\min}(\cdot)$ *denotes the minimum eigenvalue of a matrix.*

Proof. In order to proof this lemma, we consider again the general expression of any of these two matrices that is given in (40). By inserting the series expansion of $\xi(r,k)\geq 0$ in (46) into (40) we obtain an expression of $\boldsymbol{\Gamma}(\bar{\boldsymbol{\theta}})$ as a linear combination of positive semidefinite matrices with non-negative coefficients. Hence, the original covariance can be lower bounded (in the ordering of positive semidefinite matrices) by selecting any of the terms of this expansion. In the case of MUSIC we can select the term $n=0$ in (46) along the sum $k=r\geq 2$ in (40), leading to the lower bound

$$\boldsymbol{\Gamma}_{\mathrm{c}}(\bar{\boldsymbol{\theta}})\geq\sum_{k=2}^{\bar{M}}\upsilon_{\mathrm{c}}(k)\boldsymbol{A}^{\mathrm{H}}(\bar{\boldsymbol{\theta}})\boldsymbol{E}_k\boldsymbol{E}_k^{\mathrm{H}}\boldsymbol{A}(\bar{\boldsymbol{\theta}})\odot\left(\boldsymbol{A}^{\mathrm{H}}(\bar{\boldsymbol{\theta}})\boldsymbol{E}_k\boldsymbol{E}_k^{\mathrm{H}}\boldsymbol{A}(\bar{\boldsymbol{\theta}})\right)^{\mathrm{T}}$$

where

$$\upsilon_{\mathrm{c}}(k)=\left(\frac{1}{2\pi\mathrm{j}}\oint_{\mathcal{C}_z^-}\frac{\omega(z)}{z}\frac{\gamma_k}{(\gamma_k-\omega(z))^2}\mathrm{d}z\right)^2. \tag{48}$$

Likewise, for the g-MUSIC cost function we can select the term $n=1$ in (46) along the sum $k=r\geq 2$ in (40), so that

$$\boldsymbol{\Gamma}_{\mathrm{g}}(\bar{\boldsymbol{\theta}})\geq\sum_{k=2}^{\bar{M}}\upsilon_{\mathrm{g}}(k)\boldsymbol{A}^{\mathrm{H}}(\bar{\boldsymbol{\theta}})\boldsymbol{E}_k\boldsymbol{E}_k^{\mathrm{H}}\boldsymbol{A}(\bar{\boldsymbol{\theta}})\odot\left(\boldsymbol{A}^{\mathrm{H}}(\bar{\boldsymbol{\theta}})\boldsymbol{E}_k\boldsymbol{E}_k^{\mathrm{H}}\boldsymbol{A}(\bar{\boldsymbol{\theta}})\right)^{\mathrm{T}}$$

where now

$$\upsilon_{\mathrm{g}}(k)=\frac{1}{N}\sum_{j=1}^{\bar{M}}K_j\gamma_j^2\left(\frac{1}{2\pi\mathrm{j}}\oint_{\mathcal{C}_\omega^-}\frac{\omega}{z(\omega)}\frac{\gamma_k}{(\gamma_k-\omega)^2(\gamma_j-\omega)}\mathrm{d}\omega\right)^2. \tag{49}$$

Using the fact that, for any two positive semidefinite matrices $\boldsymbol{A},\boldsymbol{B}$, we have $\lambda_{\min}(\boldsymbol{A}\odot\boldsymbol{B})\geq\lambda_{\min}(\boldsymbol{A})\lambda_{\min}(\boldsymbol{B})$ [44], we see that the lemma will follow from Assumption 4 if we are able to show that $\inf_{M,k\geq 2}\upsilon_{\mathrm{c}}(k)>0$ and $\inf_{M,k\geq 2}\upsilon_{\mathrm{g}}(k)>0$.

In the case of $\upsilon_{\mathrm{g}}(k)$ in (49), we have

$$\upsilon_{\mathrm{g}}(k)=\frac{K_1}{N}\frac{\gamma_1^2\gamma_k^2}{(\gamma_1-\gamma_k)^4}\delta_{k\geq 2}+\frac{1}{N}\sum_{j=2}^{\bar{M}}K_j\frac{\gamma_j^2\gamma_k^2}{(\gamma_1-\gamma_j)^4}\delta_{k=1}\geq\frac{K_1}{N}\frac{\gamma_1^4}{(2\|\boldsymbol{R}\|)^4}\delta_{k\geq 2}+\frac{M-K_1}{N}\frac{\gamma_1^4}{(2\|\boldsymbol{R}\|)^4}\delta_{k=1}$$

and the lower bound follows from the fact that $\inf_M\gamma_1>0$, $\sup_M\|\boldsymbol{R}\|<\infty$ and $0<\inf_M K_1/M\leq\sup_M K_1/M<1$.

Regarding $\upsilon_{\mathrm{c}}(k)$ in (48) we have to differentiate between the over- and undersampled case. Using some algebra we obtain a closed-form expression for the oversampled case ($M\leq N$)

$$\upsilon_{\mathrm{c}}(k)=\gamma_k^2(\Phi_k(\mu_1)-\Phi_k(\gamma_1))^2\delta_{k\geq 2}+\left(\gamma_1\sum_{m=2}^{\bar{M}}(\Phi_1(\mu_m)-\Phi_1(\gamma_m))\right)^2\delta_{k=1} \tag{50}$$

and for the undersampled case ($M>N$)

$$\upsilon_{\mathrm{c}}(k)=(\gamma_k\Phi_k(\gamma_1))^2\delta_{k\geq 2}+\gamma_1^2\left(\sum_{m=1}^{\bar{M}}\Phi_1(\mu_m)-\sum_{m=2}^{\bar{M}}\Phi_1(\gamma_m)\right)^2\delta_{k=1} \tag{51}$$

where we have introduced $\Phi_k(x)=\frac{x}{(\gamma_k-x)^2}$. Consider first the oversampled case in (50) for $k\geq 2$. Since $\Phi_k(x)$ is a convex function on the region $0<x<\gamma_k$, we can upper bound $\Phi_k(\gamma_1)>\Phi_k(\mu_1)+\Phi_k'(\mu_1)(\gamma_1-\mu_1)$ where $\Phi_k'(x)$ is the derivative of $\Phi_k(x)$ w.r.t. x. This shows that

$$(\Phi_k(\gamma_1)-\Phi_k(\mu_1))^2\geq(\Phi_k'(\mu_1))^2(\gamma_1-\mu_1)^2\geq\frac{(\gamma_1-\mu_1)^2}{\gamma_k^4}\geq\frac{(\gamma_1-\mu_1)^2}{\|\boldsymbol{R}\|^4}$$

where we have used the fact that $\Phi_k'(\mu_1)\geq\Phi_k'(0)=1/\gamma_k^2$. On the other hand, to see that $\inf_M|\gamma_1-\mu_1|>0$ we simply recall from the definition of μ_1 in (14) that we can write

$$\gamma_1-\mu_1=\left(1-\frac{1}{N}\sum_{j=2}^{\bar{M}}K_j\frac{\gamma_j}{\gamma_j-\mu_1}\right)^{-1}\frac{K_1\gamma_1}{N}>\frac{K_1\gamma_1}{N}$$

where in the last equation we used the fact that $\mu_1<\gamma_1<\gamma_j$ for $j=2,...,\bar{M}$ and therefore the second term in the denominator is always positive. The fact that $\inf_M|\mu_1-\gamma_1|>0$ follows the boundedness of the spectral norm of $\boldsymbol{R}$ and Assumption 1. This proves that $v_c(k)$ in (50) for $k\geq 2$ is lower bounded by a constant independent of M.

Let us now consider the expression for $v_c(k)$ in (51) in the undersampled case for $k\geq 2$. The first term in (51) is clearly bounded below by a constant independent of M because we have $\Phi_k(\gamma_1)=\gamma_1/(\gamma_k-\gamma_1)^2>\gamma_1/(4\|\boldsymbol{R}\|^2)$. This concludes the proof of Lemma 3. ∎

VII. Simulation Results

In this Section the predicted probability of resolution in (27) is compared to the simulated one. Consider a scenario with $K=2$ sources that are located at $\boldsymbol{\theta}=[45°,50°]^{\mathrm{T}}$ and a ULA that is equipped with $M=15$ sensors. The transmitted signals are zero-mean with unit power and the SNR is given by SNR$=1/\sigma^2$. The simulations are carried out for correlated signals with correlation coefficient $\rho=0.95$ as well as uncorrelated signals. The separation boundary is defined as the lowest SNR or the smallest angular separation between both sources that provides separation between the eigenvalue cluster that is associated to the noise eigenvalue γ_1 and remaining eigenvalue clusters. Hence, the separation boundary is given by the smallest SNR or the smallest angular separation between both sources that allows to differentiate between noise and signal subspace and therefore satisfies Assumption 3. All simulations are conducted for 10000 Monte-Carlo trials.

In Figure 1 and 2 the probability of resolution is depicted for different SNRs and for $N=15$ and $N=100$ snapshots, respectively. In both scenarios our prediction of the probability of resolution in (27) is very accurate since it is very close to the simulated one. Even in case of correlated sources and limited number of snapshots the proposed forecast of the probability of resolution in (27) provides a remarkably accurate description of the threshold effect. In both scenarios the g-MUSIC DoA estimation method shows superior resolution capabilities than the conventional MUSIC technique.

In Figure 3 the probability of resolution is depicted for different angular separation $\Delta\vartheta$ between two sources. The SNR is fixed to SNR=2dB and a total of $N=15$ snapshots are considered. The transmitted signals are uncorrelated and the two sources are located at $\boldsymbol{\theta}=[45°,45°+\Delta\vartheta]^{\mathrm{T}}$ with $\Delta\vartheta\in[0.2°,10°]$. Furthermore, a ULA with $M=15$ antennas is used. It can be observed that the proposed prediction of the probability of resolution is almost identical to the actual one. Especially in difficult scenarios with low SNR and closely spaced sources g-MUSIC is superior to conventional MUSIC.

VIII. Conclusion

In this article the asymptotic stochastic behavior of the conventional MUSIC and the g-MUSIC cost function is investigated in the asymptotic regime where the number of snapshots and the number of sensors go to infinity at the

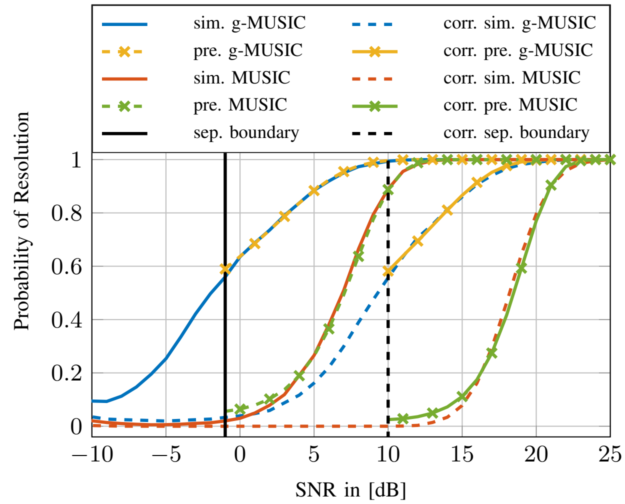

Fig. 1: Uncorrelated & Correlated Sources, Correlation Coefficient $\rho=0.95$, $M=15$ Sensors, $N=15$ Snapshots

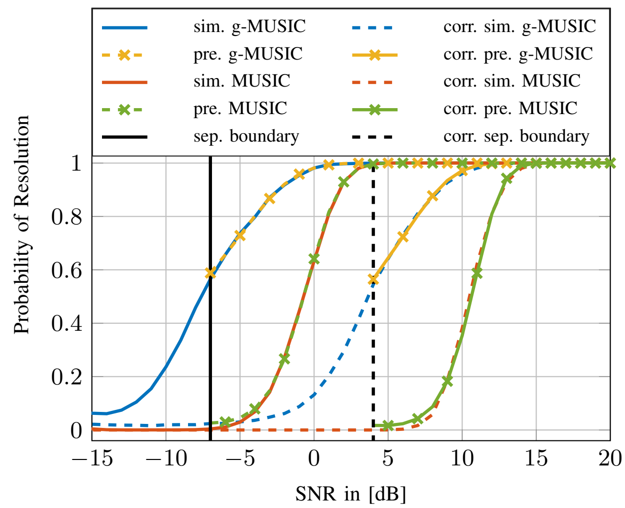

Fig. 2: Uncorrelated & Correlated Sources, Correlation Coefficient $\rho=0.95$, $M=15$ Sensors, $N=100$ Snapshots

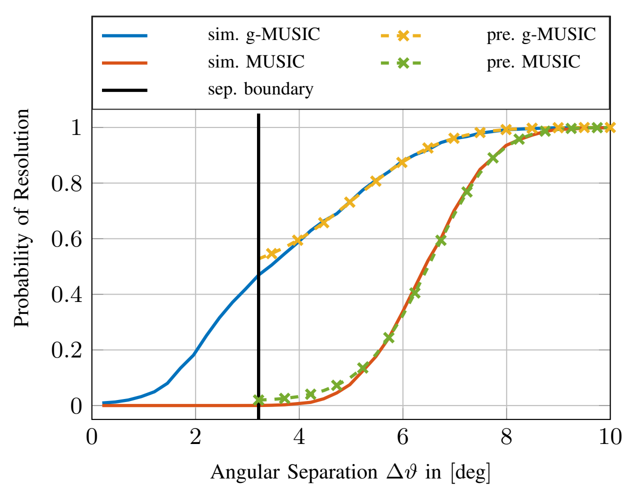

Fig. 3: Uncorrelated sources located at $\boldsymbol{\theta}=[45°,45°+\Delta\vartheta]^{\mathrm{T}}$, $M=15$ Sensors, $N=15$ Snapshots, SNR=2dB

same rate. Using tools from RMT the finite dimensional distribution of the random MUSIC and g-MUSIC cost function is derived and shown to be asymptotically jointly Gaussian distributed. Furthermore, the resolution capabilities of both MUSIC DoA estimation methods is analyzed based on the asymptotic stochastic behavior of their cost functions. An analytic expression for the probability of resolution is provided that allows to predict the probability of resolution in the threshold region.

Appendix A
Determination of the Asymptotic Covariance of the MUSIC Cost Function

In case of the conventional MUSIC cost function $\bar{h}(z(\omega_2))=1$. Hence, the complex contour integral in (42) yields

$$\mathcal{I}_{r,k}(\omega_1)=\frac{1}{2\pi\mathrm{j}}\oint_{\mathcal{C}_{\omega_2}}\frac{\omega_2}{z(\omega_2)}\frac{\partial z(\omega_2)}{\partial\omega_2}\frac{\frac{1}{(\gamma_r-\omega_2)(\gamma_k-\omega_2)}}{1-\Omega(\omega_1,\omega_2)}\mathrm{d}\omega_2 \quad (52)$$

and can be solved in closed-form by applying conventional residue calculus [45]. A closed-form expression for $\mathcal{I}_{r,k}(\omega_1)$ is obtained by summing the residues of the integrand in (52) evaluated at all singularities that lie within the complex contour $\mathcal{C}_{\omega_2}$. To begin with, we consider the oversampled case where $M\leq N$. It can be seen, that the integrand of $\mathcal{I}_{r,k}(\omega_1)$ in (52) exhibits three different types of singularities that lie inside the complex contour $\mathcal{C}_{\omega_2}$. The first type of singularities corresponds to the poles of $\frac{\omega_2}{z(\omega_2)}$, which are denoted by $\mu_1<\mu_2<\cdots<\mu_{\bar{M}}$ in (14). The corresponding residue w.r.t. ω_2 evaluated at μ_t yields

$$\mathrm{Res}\left[\frac{\omega_2}{z(\omega_2)}\frac{\partial z(\omega_2)}{\partial\omega_2}\frac{\frac{1}{(\gamma_r-\omega_2)(\gamma_k-\omega_2)}}{1-\Omega(\omega_1,\omega_2)},\,\mu_t\right]=\frac{\frac{\mu_t}{(\gamma_r-\mu_t)(\gamma_k-\mu_t)}}{1-\Omega(\omega_1,\mu_t)} \quad (53)$$

where we have used $\Omega(\omega_1,\omega_2)$ in (38), and $\frac{\partial z(\omega)}{\partial\omega}$ in (39). However, only μ_1 lies within the contour $\mathcal{C}_{\omega_2}$ which is why only the residue evaluated at μ_1 contributes to the solution of $\mathcal{I}_{r,k}(\omega_1)$ in (52).

The second type of singularities corresponds to the roots of $1-\Omega(\omega_1,\omega_2)$ where $\Omega(\omega_1,\omega_2)$ is given in (38). The complex-valued roots are denoted by $\varphi_r(\omega_1)$ for $r=1,\ldots,\bar{M}$ and sorted according to their real-part in ascending order $\mathrm{Re}[\varphi_1(\omega_1)]<\cdots<\mathrm{Re}[\varphi_{\bar{M}}(\omega_1)]$ and given by the solutions of the polynomial equation in $\varphi(\omega_1)$

$$\frac{1}{N}\sum_{l=1}^{\bar{M}}\frac{K_l\gamma_l^2}{(\gamma_l-\omega_1)(\gamma_l-\varphi(\omega_1))}=1. \quad (54)$$

The corresponding residue evaluated at $\varphi_t(\omega_1)$ is given by

$$\mathrm{Res}\left[\frac{\omega_2}{z(\omega_2)}\frac{\partial z(\omega_2)}{\partial\omega_2}\frac{\frac{1}{(\gamma_r-\omega_2)(\gamma_k-\omega_2)}}{1-\Omega(\omega_1,\omega_2)},\,\varphi_t(\omega_1)\right]$$
$$=\frac{\varphi_t(\omega_1)-\omega_1}{(\gamma_r-\varphi_t(\omega_1))(\gamma_k-\varphi_t(\omega_1))}\frac{1}{1-\frac{1}{N}\sum_{m=1}^{\bar{M}}\frac{K_m\gamma_m}{\gamma_m-\varphi_t(\omega_1)}}. \quad (55)$$

Lemma 4. *Assuming that ω_1 is located outside the contour generated by the parameterization $x\mapsto\omega_1(x)$ in [25, Remark 3], there exists exactly one solution of the equation in* (54) *that is enclosed by the contour $\mathcal{C}_{\omega_2}$, namely $\varphi_1(\omega_1)$.*

Proof. Since ω_1 is located outside the contour $\tilde{\Psi}(\omega_1)<1$ where $\tilde{\Psi}(\omega)$ is given in (44). It can be observed that for a fixed ω_1 the $\varphi_r(\omega_1)$ values are the zeros of the function $f(\varphi)=1-\Omega(\omega_1,\varphi)$ where $\Omega(\omega_1,\omega_2)$ is given in (38). By Cauchy-Schwarz inequality it follows that, if $\varphi\in\mathcal{C}_{\omega_2}$, we have $|1-f(\varphi)|^2\leq\tilde{\Psi}(\omega_1)\tilde{\Psi}(\varphi)<1$ (see Lemma 1). It can also be seen that $f(\varphi)$ has no singularities or zeros lying directly on the contour $\mathcal{C}_{\omega_2}$, so that by Rauchés's theorem $f(\varphi)$ has the same number of zeros and poles inside $\mathcal{C}_{\omega_2}$. The poles of $f(\varphi)$ are located at the true eigenvalues γ_r for $r=1,\ldots,\bar{M}$. However, only the smallest eigenvalue γ_1 is enclosed by $\mathcal{C}_{\omega_2}$. Hence, it follows that only one zero of $1-f(\varphi)$ is enclosed by the contour $\mathcal{C}_{\omega_2}$, namely $\varphi_1(\omega_1)$. ■

Consequently, only the residue evaluated at $\varphi_1(\omega_1)$ contributes to the solution of $\mathcal{I}_{r,k}(\omega_1)$ in (52).

The third type of singularities corresponds to the poles at the true eigenvalues γ_t for $t=1,\ldots,\bar{M}$. However, we have to distinguish between poles of order one and order two. The residue with respect to ω_2 evaluated at γ_t yields

$$\mathrm{Res}\left[\frac{\omega_2}{z(\omega_2)}\frac{\partial z(\omega_2)}{\partial\omega_2}\frac{\frac{1}{(\gamma_r-\omega_2)(\gamma_k-\omega_2)}}{1-\Omega(\omega_1,\omega_2)},\,\gamma_t\right]$$
$$=\begin{cases}\frac{N}{K_t\gamma_t}\frac{\gamma_t-\omega_1}{\gamma_k-\gamma_t}, & \text{for } t=r\neq k\\ \frac{N}{K_t\gamma_t}\frac{\gamma_t-\omega_1}{\gamma_r-\gamma_t}, & \text{for } t=k\neq r\\ \alpha_t(\omega_1), & \text{for } r=k=t\end{cases} \quad (56)$$

where

$$\alpha_t(\omega_1)=\frac{(\gamma_t-\omega_1)}{\left(\frac{1}{N}K_t\gamma_t\right)^2}\left(1-\frac{1}{N}\sum_{\substack{m=1\\m\neq t}}^{\bar{M}}\frac{K_m\gamma_m}{\gamma_m-\gamma_t}\right)$$
$$+\frac{(\gamma_t-\omega_1)^2}{\gamma_t\left(\frac{1}{N}K_t\gamma_t\right)^2}\left(1-\frac{1}{N}\sum_{\substack{m=1\\m\neq t}}^{\bar{M}}\frac{K_m\gamma_m^2}{(\gamma_m-\omega_1)(\gamma_m-\gamma_t)}\right). \quad (57)$$

It can be observed that only the noise eigenvalue γ_1 is enclosed by the contour $\mathcal{C}_{\omega_2}$. Correspondingly, the closed-form solution for the complex contour integral $\mathcal{I}_{r,k}(\omega_1)$ in (52) is obtained by taking the negative sum (negative sum because of the negatively orientated contour $\mathcal{C}_{\omega_2}$) of the residues in (53), (55) and (56) evaluated at all singularities that lie inside the complex contour $\mathcal{C}_{\omega_2}$ and yields

$$\mathcal{I}_{r,k}(\omega_1)=-\frac{\mu_1}{(\gamma_r-\mu_1)(\gamma_k-\mu_1)}\frac{1}{1-\Omega(\omega_1,\mu_1)}-\alpha_1(\omega_1)\delta_{r=k=1}$$
$$-\frac{\varphi_1(\omega_1)-\omega_1}{(\gamma_r-\varphi_1(\omega_1))(\gamma_k-\varphi_1(\omega_1))}\frac{1}{1-\frac{1}{N}\sum_{m=1}^{\bar{M}}\frac{K_m\gamma_m}{\gamma_m-\varphi_1(\omega_1)}}$$
$$-\frac{N}{K_1\gamma_1}\frac{\gamma_1-\omega_1}{\gamma_k-\gamma_1}\delta_{r=1\neq k}-\frac{N}{K_1\gamma_1}\frac{\gamma_1-\omega_1}{\gamma_r-\gamma_1}\delta_{k=1\neq r}. \quad (58)$$

In the following we substitute the closed-form expression for $\mathcal{I}_{r,k}(\omega_1)$ in (58) into the general expression for the real-valued weights $\xi(r,k)$ in (41)

$$\bar{\xi}_{\mathrm{c}}(r,k)=\frac{-1}{2\pi\mathrm{j}}\oint_{\mathcal{C}_{\omega_1}}\frac{\omega_1}{z(\omega_1)}\frac{\partial z(\omega_1)}{\partial\omega_1}\frac{\gamma_r\gamma_k}{(\gamma_r-\omega_1)(\gamma_k-\omega_1)}$$
$$\times\left(\alpha_1(\omega_1)\delta_{r=k=1}+\frac{\mu_1}{(\gamma_r-\mu_1)(\gamma_k-\mu_1)}\frac{1}{1-\Omega(\omega_1,\mu_1)}\right.$$
$$+\frac{N}{K_1\gamma_1}\frac{\gamma_1-\omega_1}{\gamma_k-\gamma_1}\delta_{r=1\neq k}+\frac{N}{K_1\gamma_1}\frac{\gamma_1-\omega_1}{\gamma_r-\gamma_1}\delta_{k=1\neq r} \quad (59)$$
$$\left.+\frac{\varphi_1(\omega_1)-\omega_1}{(\gamma_r-\varphi_1(\omega_1))(\gamma_k-\varphi_1(\omega_1))}\frac{1}{1-\frac{1}{N}\sum_{m=1}^{\bar{M}}\frac{K_m\gamma_m}{\gamma_m-\varphi_1(\omega_1)}}\right)\mathrm{d}\omega_1$$

where we have used $\bar{h}(z(\omega_1))=1$, $\Omega(\omega_1,\omega_2)$ in (38) and $\alpha_t(\omega_1)$ in (57). The integrand in (59) exhibits three different types of singularities. The first group of singularities corresponds to the poles that are located at the true eigenvalues γ_t. Hence, the residue of the first part of the integrand in (59) evaluated at γ_t is given by

$$\begin{aligned}&\mathrm{Res}\left[\frac{\omega_1}{z(\omega_1)}\frac{\partial z(\omega_1)}{\partial\omega_1}\frac{\alpha_t(\omega_1)}{(\gamma_r-\omega_1)(\gamma_k-\omega_1)}\delta_{r=k=t},\ \gamma_t\right]\\&=-\frac{N}{K_t}\frac{1}{\left(\frac{1}{N}K_t\gamma_t\right)^2}\left(1-\frac{1}{N}\sum_{\substack{m=1\\m\neq t}}^{\bar{M}}\frac{K_m\gamma_m}{\gamma_m-\gamma_t}\right)^2\delta_{r=k=t}\\&\quad-\frac{1}{\left(\frac{1}{N}K_t\gamma_t\right)^2}\left(1-\frac{1}{N}\sum_{\substack{m=1\\m\neq t}}^{\bar{M}}\frac{K_m\gamma_m^2}{(\gamma_m-\gamma_t)^2}\right)\delta_{r=k=t}\end{aligned}\tag{60}$$

whereas the residue of the second part of the integrand in (59) yields

$$\begin{aligned}&\mathrm{Res}\left[\frac{\frac{\mu_t}{(\gamma_r-\mu_t)(\gamma_k-\mu_t)}}{1-\Omega(\omega_1,\mu_t)}\frac{\frac{\omega_1}{z(\omega_1)}\frac{\partial z(\omega_1)}{\partial\omega_1}}{(\gamma_r-\omega_1)(\gamma_k-\omega_1)},\ \gamma_t\right]\\&=\begin{cases}\frac{1}{\frac{1}{N}K_t\gamma_t}\frac{\mu_t}{\gamma_k-\mu_t}\frac{1}{\gamma_k-\gamma_t}, & \text{for } t=r\neq k\\ \frac{1}{\frac{1}{N}K_t\gamma_t}\frac{\mu_t}{\gamma_r-\mu_t}\frac{1}{\gamma_r-\gamma_t}, & \text{for } t=k\neq r\\ \beta_t, & \text{for } t=k=r\end{cases}\end{aligned}\tag{61}$$

where

$$\begin{aligned}\beta_t=&\frac{1}{\left(\frac{1}{N}K_t\gamma_t\right)^2}\frac{\mu_t}{\gamma_t-\mu_t}\left(1-\frac{1}{N}\sum_{\substack{m=1\\m\neq t}}^{\bar{M}}\frac{K_m\gamma_m}{\gamma_m-\gamma_t}\right)\\&+\frac{\mu_t}{\gamma_t\left(\frac{1}{N}K_t\gamma_t\right)^2}\left(1-\frac{1}{N}\sum_{\substack{m=1\\m\neq t}}^{\bar{M}}\frac{K_m\gamma_m^2}{(\gamma_m-\gamma_t)(\gamma_m-\mu_t)}\right).\end{aligned}$$

The residue of the third part of the integrand in (59) evaluated at γ_t is computed as follows

$$\begin{aligned}&\mathrm{Res}\left[\frac{N}{K_t\gamma_t}\frac{\omega_1}{z(\omega_1)}\frac{\partial z(\omega_1)}{\partial\omega_1}\frac{\frac{\gamma_t-\omega_1}{\gamma_k-\gamma_t}\delta_{r=t\neq k}+\frac{\gamma_t-\omega_1}{\gamma_r-\gamma_t}\delta_{k=t\neq r}}{(\gamma_r-\omega_1)(\gamma_k-\omega_1)},\ \gamma_t\right]\\&=-\frac{N}{K_t}\frac{1}{(\gamma_k-\gamma_t)^2}\delta_{r=t\neq k}-\frac{N}{K_t}\frac{1}{(\gamma_r-\gamma_t)^2}\delta_{k=t\neq r}.\end{aligned}\tag{62}$$

Since only the noise eigenvalue γ_1 is enclosed by the contour $\mathcal{C}_{\omega_1}$, only the residues in (60), (61) and (62) evaluated at γ_1 contribute to the result of $\bar{\xi}_{\mathrm{c}}(r,k)$ in (59).

The second type of singularities belongs to the poles of $\frac{\omega_1}{z(\omega_1)}$, which are located at the μ-values that are defined in (14). The corresponding residue of the first part of the integrand in (59) evaluated at μ_t is given by

$$\begin{aligned}&\mathrm{Res}\left[\frac{\omega_1}{z(\omega_1)}\frac{\partial z(\omega_1)}{\partial\omega_1}\frac{\alpha_t(\omega_1)}{(\gamma_r-\omega_1)(\gamma_k-\omega_1)}\delta_{r=k=t},\ \mu_t\right]\\&=\frac{\mu_t}{\gamma_t-\mu_t}\frac{1}{\left(\frac{1}{N}K_t\gamma_t\right)^2}\left(1-\frac{1}{N}\sum_{\substack{m=1\\m\neq t}}^{\bar{M}}\frac{K_m\gamma_m}{\gamma_m-\gamma_t}\right)\delta_{r=k=t}\\&\quad+\frac{\mu_t}{\gamma_t\left(\frac{1}{N}K_t\gamma_t\right)^2}\left(1-\frac{1}{N}\sum_{\substack{m=1\\m\neq t}}^{\bar{M}}\frac{K_m\gamma_m^2}{(\gamma_m-\mu_t)(\gamma_m-\gamma_t)}\right)\delta_{r=k=t}.\end{aligned}\tag{63}$$

Furthermore, the residues of the second and third part of the integrand in (59) evaluated at μ_t are given by

$$\begin{aligned}&\mathrm{Res}\left[\frac{\frac{\mu_t}{(\gamma_r-\mu_t)(\gamma_k-\mu_t)}}{1-\Omega(\omega_1,\mu_t)}\frac{\frac{\omega_1}{z(\omega_1)}\frac{\partial z(\omega_1)}{\partial\omega_1}}{(\gamma_r-\omega_1)(\gamma_k-\omega_1)},\ \mu_t\right]\\&=\frac{\mu_t^2}{(\gamma_r-\mu_t)^2(\gamma_k-\mu_t)^2}\frac{1}{\left(1-\frac{1}{N}\sum_{m=1}^{\bar{M}}\frac{K_m\gamma_m^2}{(\gamma_m-\mu_t)^2}\right)}\end{aligned}\tag{64}$$

and

$$\begin{aligned}&\mathrm{Res}\left[\frac{N}{K_t\gamma_t}\frac{\omega_1}{z(\omega_1)}\frac{\partial z(\omega_1)}{\partial\omega_1}\frac{\frac{\gamma_t-\omega_1}{\gamma_k-\gamma_t}\delta_{r=t\neq k}+\frac{\gamma_t-\omega_1}{\gamma_r-\gamma_t}\delta_{k=t\neq r}}{(\gamma_r-\omega_1)(\gamma_k-\omega_1)},\ \mu_t\right]\\&=\frac{N}{K_t}\frac{1}{(\gamma_k-\gamma_t)\gamma_t}\frac{\mu_t}{\gamma_k-\mu_t}\delta_{r=t\neq k}+\frac{N}{K_t}\frac{1}{(\gamma_r-\gamma_t)\gamma_t}\frac{\mu_t}{\gamma_r-\mu_t}\delta_{k=t\neq r}.\end{aligned}\tag{65}$$

However, only μ_1 is enclosed by the contour $\mathcal{C}_{\omega_1}$ which is why only the residues in (63), (64) and (65) evaluated at μ_1 contribute to the final result of $\bar{\xi}_{\mathrm{c}}(r,k)$ in (59).

The third type of singularities of the integrand in (59) is given by the solutions to the polynomial equation $1=\Omega(\omega_1,\mu_t)$ in ω_1 where $\Omega(\omega_1,\omega_2)$ is defined in (38). However, using Cauchy's argument principle it can be shown that the solutions to $1=\Omega(\omega_1,\mu_t)$ are located outside the contour $\mathcal{C}_{\omega_1}$ and therefore do not contribute to the solution of $\bar{\xi}_{\mathrm{c}}(r,k)$ in (59). The following lemma is in line.

Lemma 5. *Function $f(\omega_1)=1-\Omega(\omega_1,\mu_t)$ with $\Omega(\omega_1,\omega_2)$ in* (38) *does not exhibit any zeros inside the contour $\mathcal{C}_{\omega_1}$.*

Proof. Let P denote the number of poles and Z the number of zeros of $f(\omega_1)$ that are located inside the contour $\mathcal{C}_{\omega_1}$, then according to Cauchy's argument principle

$$-\frac{1}{2\pi\mathrm{j}}\oint_{\mathcal{C}_{\omega_1}}\frac{f'(\omega_1)}{f(\omega_1)}\mathrm{d}\omega_1=Z-P,\tag{66}$$

where the first order derivative of $f(\omega_1)$ w.r.t. ω_1 is given by

$$f'(\omega_1)=\frac{\partial f(\omega_1)}{\partial\omega_1}=-\frac{1}{N}\sum_{m=1}^{\bar{M}}\frac{K_m\gamma_m^2}{(\gamma_m-\omega_1)^2(\gamma_m-\mu_t)}.\tag{67}$$

Substituting $f(\omega_1)=1-\Omega(\omega_1,\mu_t)$ and its first oder derivative in (67) into the argument principle in (66) yields

$$\begin{aligned}&\frac{1}{2\pi\mathrm{j}}\oint_{\mathcal{C}_{\omega_1}}\frac{\frac{1}{N}\sum_{m=1}^{\bar{M}}\frac{K_m\gamma_m^2+\gamma_m-\gamma_m}{(\gamma_m-\omega_1)^2(\gamma_m-\mu_t)}}{1-\frac{1}{N}\sum_{m=1}^{\bar{M}}\frac{K_m\gamma_m^2}{(\gamma_m-\omega_1)(\gamma_m-\mu_t)}}\frac{\mu_t-\omega_1}{\mu_t-\omega_1}\mathrm{d}\omega_1\\&=\frac{1}{2\pi\mathrm{j}}\oint_{\mathcal{C}_{\omega_1}}\frac{1}{\mu_t-\omega_1}\frac{\frac{1}{N}\sum_{m=1}^{\bar{M}}\frac{K_m\gamma_m^2(\mu_t-\gamma_m)}{(\gamma_m-\omega_1)^2(\gamma_m-\mu_t)}}{1-\frac{1}{N}\sum_{m=1}^{\bar{M}}\frac{K_m\gamma_m^2}{(\gamma_m-\omega_1)(\gamma_m-\mu_t)}}\mathrm{d}\omega_1\\&\quad+\frac{1}{2\pi\mathrm{j}}\oint_{\mathcal{C}_{\omega_1}}\frac{1}{\mu_t-\omega_1}\frac{\frac{1}{N}\sum_{m=1}^{\bar{M}}\frac{K_m\gamma_m^2(\gamma_m-\omega_1)}{(\gamma_m-\omega_1)^2(\gamma_m-\mu_t)}}{1-\frac{1}{N}\sum_{m=1}^{\bar{M}}\frac{K_m\gamma_m^2}{(\gamma_m-\omega_1)(\gamma_m-\mu_t)}}\mathrm{d}\omega_1\end{aligned}$$

where we have added and subtracted γ_m and multiplied and divided by $\mu_t-\omega_1$. Next, we add and subtract 1 to obtain

$$\begin{aligned}&\frac{1}{2\pi\mathrm{j}}\oint_{\mathcal{C}_{\omega_1}}\frac{1}{\mu_t-\omega_1}\frac{1-\frac{1}{N}\sum_{m=1}^{\bar{M}}\frac{K_m\gamma_m^2}{(\gamma_m-\omega_1)^2}}{1-\frac{1}{N}\sum_{m=1}^{\bar{M}}\frac{K_m\gamma_m^2}{(\gamma_m-\omega_1)(\gamma_m-\mu_t)}}\mathrm{d}\omega_1\\&+\frac{1}{2\pi\mathrm{j}}\oint_{\mathcal{C}_{\omega_1}}\frac{1}{\mu_t-\omega_1}\frac{\frac{1}{N}\sum_{m=1}^{\bar{M}}\frac{K_m\gamma_m^2}{(\gamma_m-\omega_1)(\gamma_m-\mu_t)}-1}{1-\frac{1}{N}\sum_{m=1}^{\bar{M}}\frac{K_m\gamma_m^2}{(\gamma_m-\omega_1)(\gamma_m-\mu_t)}}\mathrm{d}\omega_1\\&=\frac{1}{2\pi\mathrm{j}}\oint_{\mathcal{C}_{\omega_1}}\left[\frac{1}{z_1}\left(1-\frac{1}{N}\sum_{m=1}^{\bar{M}}\frac{K_m\gamma_m^2}{(\gamma_m-\omega_1)^2}\right)-\frac{1}{\mu_t-\omega_1}\right]\mathrm{d}\omega_1\end{aligned}\tag{68}$$

where we have used

$$z_1=(\omega_1-\mu_t)\left[1-\frac{1}{N}\sum_{m=1}^{\bar{M}}\frac{K_m\gamma_m^2}{(\gamma_m-\omega_1)(\gamma_m-\mu_t)}\right]$$

which follows by subtracting $0=\mu_t\left(1-\frac{1}{N}\sum_{m=1}^{\bar{M}}\frac{K_m\gamma_m}{\gamma_m-\mu_t}\right)$ from the definition of z_1 in (17). Applying the change of variables $\mathrm{d}\omega_1=\frac{\partial\omega(z_1)}{\partial z_1}\mathrm{d}z_1$ in (68) one obtains

$$\frac{1}{2\pi\mathrm{j}}\oint_{\mathcal{C}_{z_1}}\frac{1}{z_1}\mathrm{d}z_1-\frac{1}{2\pi\mathrm{j}}\oint_{\mathcal{C}_{\omega_1}}\frac{1}{\mu_t-\omega_1}\mathrm{d}\omega_1=\mathrm{Res}\left[\frac{1}{\mu_t-\omega_1},\ \mu_t\right]=-1$$

for (66). Furthermore, it can be observed that $f(\omega_1)$ exhibits a single pole that is located inside the contour $\mathcal{C}_{\omega_1}$ such that $P=1$. Consequently, $Z=0$ and no zero of $f(\omega_1)$ is located inside the contour $\mathcal{C}_{\omega_1}$. ■

It remains to compute the complex contour integral that belongs to the last part in (59). By applying the change of variables $\mathrm{d}\omega_1=\frac{\partial\omega(z_1)}{\partial z_1}\mathrm{d}z_1$ and parameterizing the complex contour as proposed in [25, Section IV] it can be shown that the complex contour integral simplifies to a real-valued integral

$$\frac{-1}{2\pi \mathrm{j}}\oint_{\mathcal{C}_{\omega_1}} \frac{(\varphi_1(\omega_1){-}\omega_1)\frac{\omega_1}{z(\omega_1)}\frac{\partial z(\omega_1)}{\partial\omega_1}\frac{1}{(\gamma_r-\omega_1)(\gamma_k-\omega_1)}}{(\gamma_r{-}\varphi_1(\omega_1))(\gamma_k{-}\varphi_1(\omega_1))\left(1{-}\frac{1}{N}\sum_{m=1}^{\bar{M}}\frac{K_m\gamma_m}{\gamma_m-\varphi_1(\omega_1)}\right)}\mathrm{d}\omega_1$$
$$=\frac{2}{\pi}\int_{x_1^-}^{x_1^+}\frac{1}{\left|1{-}\frac{1}{N}\sum_{m=1}^{\bar{M}}\frac{K_m\gamma_m}{\gamma_m-\omega(x)}\right|^2}\frac{\mathrm{Im}[\omega(x)]}{\left|\gamma_r{-}\omega(x)\right|^2\left|\gamma_k{-}\omega(x)\right|^2}\mathrm{d}x \tag{69}$$

which can be solved numerically. The following lemma was used to simplify the real-valued integral.

Lemma 6. *By parameterizing the contour $\mathcal{C}_{\omega_1}$ as proposed in [25, Section IV]*

$$\frac{1}{N}\sum_{r=1}^{\bar{M}}\frac{K_r\gamma_r^2}{|\gamma_r{-}\omega(x)|^2}{=}1 \tag{70}$$

for $x{\in}\mathcal{S}$ and it can be shown that

$$\lim_{\omega_1\to\omega(x)}\varphi_t(\omega_1){=}\omega(x)^*,\quad \textit{for } x{\in}[x_t^-,x_t^+]. \tag{71}$$

Proof. Let $u(x)$ and $v(x)$ denote the real and imaginary parts of $\omega(x)$ in (17), i.e., $\omega(x){=}u(x){+}\mathrm{j}v(x)$. It is shown in [24, Proposition 2] that $v(x){>}0$ for $x{\in}\mathring{\mathcal{S}}{\equiv}(x_1^-,x_1^+){\cup}{\cdots}{\cup}(x_S^-,x_S^+)$. Taking imaginary parts on both sides of (17) one obtains

$$0{=}v(x)\left(1{-}\frac{1}{N}\sum_{r=1}^{\bar{M}}\frac{K_r\gamma_r^2}{(\gamma_r{-}u(x))^2{+}v(x)^2}\right)$$

which implies that

$$1{=}\frac{1}{N}\sum_{r=1}^{\bar{M}}\frac{K_r\gamma_r^2}{(\gamma_r{-}u(x))^2{+}v(x)^2}{=}\frac{1}{N}\sum_{r=1}^{\bar{M}}\frac{K_r\gamma_r^2}{|\gamma_r{-}\omega(x)|^2} \tag{72}$$

for $x{\in}\mathring{\mathcal{S}}$. From [25, Proposition 1] it follows that (72) also holds for the boundaries of the clusters $x{\in}\{x_1^-,x_1^+,...,x_S^-,x_S^+\}$. Furthermore, the convergence result in (71) follows as a direct consequence of (70) and the definition of $\varphi_t(\omega_1)$ in (54). ■

The final expression for the weights $\bar{\xi}_{\mathrm{c}}(r,k)$ in (22) in the oversampled case where $M{\le}N$ is obtained by taking the sum of the residues in (60), (61), (62), (63), (64), (65) evaluated at all singularities that lie inside the contour $\mathcal{C}_{\omega_1}$ and adding (69), which can be evaluated numerically.

In the undersampled case where $M{>}N$ it can be observed that the poles of $\frac{\omega}{z(\omega)}$ are not enclosed by any of the two contours $\mathcal{C}_{\omega_1}$ and $\mathcal{C}_{\omega_2}$. Hence, the weights $\bar{\xi}_{\mathrm{c}}(r,k)$ in (21) are obtained by discarding all residues evaluated at μ_1.

Appendix B
Determination of the asymptotic covariance of the g-MUSIC cost function

In case of the g-MUSIC cost function $\bar{h}(z(\omega_2)){=}\frac{z(\omega_2)}{\omega_2}\frac{\partial\omega(z_2)}{\partial z_2}$. Hence the complex contour integral in (42) simplifies as follows

$$\mathcal{I}_{r,k}(\omega_1){=}\frac{1}{2\pi\mathrm{j}}\oint_{\mathcal{C}_{\omega_2}}\frac{1}{(\gamma_r{-}\omega_2)(\gamma_k{-}\omega_2)}\frac{1}{1{-}\Omega(\omega_1,\omega_2)}\mathrm{d}\omega_2 \tag{73}$$

which can be solved in closed-form using conventional residue calculus [45]. It can be observed that the integrand in (73) exhibits two different types of singularities. The first type of singularities belongs to the roots of $1{-}\Omega(\omega_1,\omega_2)$ where $\Omega(\omega_1,\omega_2)$ is given in (38). The complex-valued roots are denoted by $\varphi_t(\omega_1)$ for $t{=}1,...,\bar{M}$ and defined in (54). The residue w.r.t. ω_2 evaluated at $\varphi_t(\omega_1)$ is given by

$$\mathrm{Res}\left[\frac{\frac{1}{(\gamma_r-\omega_2)(\gamma_k-\omega_2)}}{1{-}\Omega(\omega_1,\omega_2)},\,\varphi_t(\omega_1)\right]{=}\frac{\frac{-1}{(\gamma_r-\varphi_t(\omega_1))(\gamma_k-\varphi_t(\omega_1))}}{\frac{1}{N}\sum_{r=1}^{\bar{M}}\frac{K_r\gamma_r^2}{(\gamma_r-\omega_1)(\gamma_r-\varphi_t(\omega_1))^2}}. \tag{74}$$

However, it can be seen that only the residue evaluated at $\varphi_1(\omega_1)$ contributes to the solution of $\mathcal{I}_{r,k}(\omega_1)$ in (73) as it is the only singularity of the roots of $1{-}\Omega(\omega_1,\omega_2)$ that is enclosed by the contour $\mathcal{C}_{\omega_2}$.

The second type of singularities belongs to the poles of the integrand in (73) at γ_t for $t{=}1,...,\bar{M}$. The corresponding residue w.r.t. ω_2 evaluated at γ_t is given by

$$\mathrm{Res}\left[\frac{\frac{1}{(\gamma_r-\omega_2)(\gamma_k-\omega_2)}}{1{-}\Omega(\omega_1,\omega_2)},\,\gamma_t\right]{=}\begin{cases}\frac{\gamma_t-\omega_1}{\frac{1}{N}K_t\gamma_t^2} & \text{for } r{=}k{=}t\\ 0 & \text{for } r{\neq}k.\end{cases} \tag{75}$$

It can be observed that only the first eigenvalue γ_1 is enclosed by the contour $\mathcal{C}_{\omega_2}$. Hence, only the residue evaluated at γ_1 contributes to the closed-form expression of $\mathcal{I}_{r,k}(\omega_1)$ in (73) which is obtained by taking the negative sum (negative due to the negatively orientated contour) of the residue in (74) evaluated at $\varphi_1(\omega_1)$ and the residue in (75) evaluated at γ_1

$$\mathcal{I}_{r,k}(\omega_1){=}\frac{\frac{1}{(\gamma_r-\varphi_1(\omega_1))(\gamma_k-\varphi_1(\omega_1))}}{\frac{1}{N}\sum_{r=1}^{\bar{M}}\frac{K_r\gamma_r^2}{(\gamma_r-\omega_1)(\gamma_r-\varphi_1(\omega_1))^2}}-\frac{\gamma_1{-}\omega_1}{\frac{1}{N}K_1\gamma_1^2}. \tag{76}$$

Substituting the closed-form expression for $\mathcal{I}_{r,k}(\omega_1)$ in (76) into the general expression of $\xi_{\mathrm{g}}(r,k)$ in (41) and using $\bar{h}(z(\omega_1)){=}\frac{z(\omega_1)}{\omega_1}\frac{\partial\omega(z_1)}{\partial z_1}$ yields

$$\xi_{\mathrm{g}}(r,k){=}\frac{1}{2\pi\mathrm{j}}\oint_{\mathcal{C}_{\omega_1}}\frac{\frac{\gamma_r\gamma_k}{(\gamma_r-\omega_1)(\gamma_k-\omega_1)(\gamma_r-\varphi_1(\omega_1))(\gamma_k-\varphi_1(\omega_1))}}{\frac{1}{N}\sum_{m=1}^{\bar{M}}\frac{K_m\gamma_m^2}{(\gamma_m-\omega_1)(\gamma_m-\varphi_1(\omega_1))^2}}\mathrm{d}\omega_1$$
$$-\frac{1}{2\pi\mathrm{j}}\oint_{\mathcal{C}_{\omega_1}}\frac{1}{(\gamma_r{-}\omega_1)(\gamma_k{-}\omega_1)}\frac{\gamma_1{-}\omega_1}{\frac{1}{N}K_1\gamma_1^2}\mathrm{d}\omega_1. \tag{77}$$

It can be observed that the integrand of the second contour integral in (77) exhibits a single singularity at γ_1 that lies within the contour $\mathcal{C}_{\omega_1}$. The corresponding residue w.r.t. ω_1 evaluated at γ_1 is given by

$$\mathrm{Res}\left[\frac{(\gamma_t{-}\omega_1)\frac{1}{\frac{1}{N}K_t\gamma_t^2}}{(\gamma_r{-}\omega_1)(\gamma_k{-}\omega_1)},\,\gamma_t\right]{=}\begin{cases}\frac{-1}{\frac{1}{N}K_t\gamma_t^2}, & \text{for } r{=}k{=}t\\ 0, & r{\neq}k.\end{cases} \tag{78}$$

Hence the closed-form solution for the second integral in (77) is given by the residue in (78) evaluated at γ_1 for $r{=}k{=}1$ or zero otherwise. The first contour integral in (77) can be solved numerically by applying the change of variables $\mathrm{d}\omega{=}\frac{\partial\omega(x)}{\partial x}\mathrm{d}x$ and parameterizing the contour $\mathcal{C}_{\omega_1}$ by concatenation of $\omega(x)$ and $\omega(x)^*$ as proposed in [25, Section IV] such that

$$\frac{1}{2\pi\mathrm{j}}\oint_{\mathcal{C}_{\omega_1}}\frac{\frac{1}{(\gamma_r-\omega_1)(\gamma_k-\omega_1)(\gamma_r-\varphi_1(\omega_1))(\gamma_k-\varphi_1(\omega_1))}}{\frac{1}{N}\sum_{m=1}^{\bar{M}}\frac{K_m\gamma_m^2}{(\gamma_m-\omega_1)(\gamma_m-\varphi_1(\omega_1))^2}}\mathrm{d}\omega_1$$
$$=\frac{1}{\pi}\int_{x_1^-}^{x_1^+}\mathrm{Im}\left[\frac{\frac{1}{|\gamma_r-\omega(x)|^2|\gamma_k-\omega(x)|^2}}{\frac{1}{N}\sum_{r=1}^{\bar{M}}\frac{K_r\gamma_r^2}{|\gamma_r-\omega(x)|^2(\gamma_r-\omega(x)^*)}}\frac{\partial\omega(x)}{\partial x}\right]\mathrm{d}x \tag{79}$$

where we have used Lemma 6 to simplify the expression. The following Lemma allows to further simplify the real-valued integral in (79).

Lemma 7. *By parameterizing the contour $\mathcal{C}_\omega$ through concatenation of $\omega(x)$ in* (17) *and $\omega(x)^*$ as proposed in [25, Section IV] the following equality holds*

$$\frac{1}{N}\sum_{r=1}^{\bar{M}}\frac{K_r\gamma_r^2}{|\gamma_r{-}\omega(x)|^2(\gamma_r{-}\omega(x))^*}{=}\frac{1}{2\mathrm{j}\mathrm{Im}[\omega(x)]\omega'(x)^*} \tag{80}$$

where $\omega'(x)$ is defined in (18).

Proof. Let $u(x)$ and $v(x)$ denote the real and imaginary parts of $\omega(x)$ in (17), i.e., $\omega(x){=}u(x){+}\mathrm{j}v(x)$. Using the expression in (70) we can express the inverse of the first order derivative of $\omega(x)$ with respect to x in (18) as

$$\frac{1}{\omega'(x)}=\frac{1}{N}\sum_{r=1}^{\bar{M}}\frac{K_r\gamma_r^2[(\gamma_r-\omega(x))^2-|\gamma_r-\omega(x)|^2]}{(\gamma_r-\omega(x))^2|\gamma_r-\omega(x)|^2} \quad (81)$$

$$=\frac{1}{N}\sum_{r=1}^{\bar{M}}\frac{-K_r\gamma_r^2[2\mathrm{j}v(x)(\gamma_r-u(x))+2v(x)^2]}{|\gamma_r-\omega(x)|^2[(\gamma_r-u(x))^2-v(x)^2-2\mathrm{j}v(x)(\gamma_r-u(x))]}.$$

Taking the complex conjugate of $\frac{1}{\omega'(x)}$ in (81) and multiplying by $\frac{1}{2\mathrm{j}v(x)}$ one obtains the following expression for $\frac{1}{2\mathrm{j}v(x)\omega'(x)^*}$

$$\frac{1}{N}\sum_{r=1}^{\bar{M}}\frac{K_r\gamma_r^2[(\gamma_r-u(x))+\mathrm{j}v(x)]}{|\gamma_r-\omega(x)|^2[(\gamma_r-u(x))^2+2\mathrm{j}v(x)(\gamma_r-u(x))-v(x)^2]}$$

which is identical to the one in (80). ∎

Using the equalities established in (80) the real-valued integral in (79) can equivalently be expressed as

$$\frac{2}{\pi}\int_{x_1^-}^{x_1^+}\frac{|\omega'(x)|^2\mathrm{Im}[\omega(x)]}{|\gamma_r-\omega(x)|^2|\gamma_k-\omega(x)|^2}\mathrm{d}x. \quad (82)$$

Finally, the solution for $\xi_{\mathrm{g}}(r,k)$ in (24) is obtained by summing the residue in (78) for $t=1$ and (82).

References

[1] A. M. Rembovsky, A. V. Ashikhmin, V. A. Kozmin, and S. Smolskiy, *Radio Monitoring: Problems, Methods and Equipment*, ser. Lecture Notes in Electrical Engineering. Springer US, 2009.

[2] H. V. Trees, *Optimum Array Processing: Detection, Estimation, and Modulation Theory*, ser. Detection, Estimation, and Modulation Theory. Wiley, 2004.

[3] H. Krim and M. Viberg, "Two Decades of Array Signal Processing Research: The Parametric Approach," *IEEE Signal Processing Magazine*, vol. 13, no. 4, pp. 67–94, 1996.

[4] P.-J. Chung, M. Viberg, and J. Yu, "DOA Estimation Methods and Algorithms," in *Academic Press Library in Signal Processing*. Elsevier, 2014, vol. 3, pp. 599 – 650.

[5] R. Schmidt, "Multiple Emitter Location and Signal Parameter Estimation," *IEEE Transactions on Antennas and Propagation*, vol. 34, no. 3, pp. 276–280, 1986.

[6] X. Mestre and M. A. Lagunas, "Modified Subspace Algorithms for DoA Estimation With Large Arrays," *IEEE Transactions on Signal Processing*, vol. 56, no. 2, pp. 598–614, 2008.

[7] F. Athley, "Threshold Region Performance of Maximum Likelihood Direction of Arrival Estimators," *IEEE Transactions on Signal Processing*, vol. 53, no. 4, pp. 1359–1373, 2005.

[8] M. Kaveh and A. Barabell, "The Statistical Performance of the MUSIC and the Minimum-Norm Algorithms in Resolving Plane Waves in Noise," *IEEE Transactions on Acoustics, Speech, and Signal Processing*, vol. 34, no. 2, pp. 331–341, 1986.

[9] B. Porat and B. Friedlander, "Analysis of the Asymptotic Relative Efficiency of the MUSIC Algorithm," *IEEE Transactions on Acoustics, Speech, and Signal Processing*, vol. 36, no. 4, pp. 532–544, 1988.

[10] P. Stoica and A. Nehorai, "MUSIC, Maximum Likelihood and Cramér-Rao Bound," *IEEE Transactions on Acoustics, Speech, and Signal Processing*, vol. 37, no. 5, pp. 720–741, 1989.

[11] ——, "MUSIC, Maximum Likelihood and Cramér-Rao Bound: Further Results and Comparisons," 1989, pp. 2605–2608 vol.4.

[12] H. B. Lee and M. S. Wengrovitz, "Statistical Characterization of the MUSIC Null Spectrum," *IEEE Transactions on Signal Processing*, vol. 39, no. 6, pp. 1333–1347, 1991.

[13] Xiao-Liang Yu and K. M. Buckley, "Bias and Variance of Direction-of-Arrival Estimates from MUSIC, MIN-NORM, and FINE," *IEEE Transactions on Signal Processing*, vol. 42, no. 7, pp. 1812–1816, 1994.

[14] B. M. Radich and K. M. Buckley, "The Effect of Source Number Underestimation on MUSIC Location Estimates," *IEEE Transactions on Signal Processing*, vol. 42, no. 1, pp. 233–236, 1994.

[15] P. Vallet, X. Mestre, and P. Loubaton, "Performance Analysis of an Improved MUSIC DoA Estimator," *IEEE Transactions on Signal Processing*, vol. 63, no. 23, pp. 6407–6422, 2015.

[16] D. Schenck, X. Mestre, and M. Pesavento, "Probability of Resolution of Partially Relaxed Deterministic Maximum Likelihood: An Asymptotic Approach," *IEEE Transactions on Signal Processing*, 2020.

[17] ——, "Probability of Resolution of Partially Relaxed DML an Asymptotic Approach," *IEEE International Workshop on Computational Advances in Multi-Sensor Adaptive Processing*, pp. 410–414, 2019.

[18] ——, "Asymptotic Stochastic Analysis of Partially Relaxed DML," *IEEE International Conference on Acoustics, Speech and Signal Processing*, pp. 4920–4924, 2020.

[19] X. Mestre and P. Vallet, "On the Resolution Probability of Conditional and Unconditional Maximum Likelihood DoA Estimation," *IEEE Transactions on Signal Processing*, vol. 68, pp. 4656–4671, 2020.

[20] X. Mestre, P. Vallet, and P. Loubaton, "On the Resolution Probability of Conditional and Unconditional Maximum Likelihood DOA Estimation," *European Signal Processing Conference*, 2013.

[21] D. Schenck, X. Mestre, and M. Pesavento, "Probability of Resolution of G-MUSIC: An Asymptotic Approach," *IEEE International Conference on Acoustics, Speech and Signal Processing*, pp. 4360–4364, 2021.

[22] J. W. Silverstein, "Strong Convergence of the Empirical Distribution of Eigenvalues of Large Dimensional Random Matrices," *Journal of Multivariate Analysis*, vol. 55, no. 2, pp. 331–339, 1995.

[23] V. L. Girko, "Strong Law for the Eigenvalues and Eigenvectors of Empirical Covariance Matrices," *Random Operators and Stochastic Equations*, vol. 4, no. 2, pp. 179–204, 1996.

[24] X. Mestre, "On the Asymptotic Behavior of the Sample Estimates of Eigenvalues and Eigenvectors of Covariance Matrices," *IEEE Transactions on Signal Processing*, vol. 56, no. 11, pp. 5353 – 5368, 2008.

[25] ——, "Improved Estimation of Eigenvalues and Eigenvectors of Covariance Matrices Using Their Sample Estimates," *IEEE Transactions on Information Theory*, vol. 54, no. 11, pp. 5113–5129, 2008.

[26] Z. D. Bai and J. W. Silverstein, "No Eigenvalues Outside the Support of the Limiting Spectral Distribution of Large-Dimensional Sample Covariance Matrices," *The Annals of Probability*, vol. 26, no. 1, pp. 316–345, 1998.

[27] J. W. Silverstein and S. I. Choi, "Analysis of the Limiting Spectral Distribution of Large Dimensional Random Matrices," *Journal of Multivariate Analysis*, vol. 54, no. 2, pp. 295 – 309, 1995.

[28] D. Rife and R. Boorstyn, "Single-Tone Parameter Estimation from Discrete-Time Observations," *IEEE Transactions on Information Theory*, vol. 20, no. 5, pp. 591–598, 1974.

[29] H. Cox, "Resolving Power and Sensitivity to Mismatch of Optimum Array Processors," *The Journal of the Acoustical Society of America*, vol. 54, no. 3, pp. 771–785, 1973.

[30] P. Stoica, V. Šimonytė, and T. Söderström, "On the resolution performance of spectral analysis," *Signal Processing*, vol. 44, no. 2, pp. 153–161, 1995.

[31] P. Stoica and A. Gershman, "Maximum-Likelihood DOA Estimation by Data-Supported Grid Search," *IEEE Signal Processing Letters*, vol. 6, no. 10, pp. 273–275, 1999.

[32] Q. T. Zhang, "Probability of Resolution of the MUSIC Algorithm," *IEEE Transactions on Signal Processing*, vol. 43, no. 4, pp. 978–987, 1995.

[33] A. Genz, "Numerical Computation of Multivariate Normal Probabilities," *Journal of Computational and Graphical Statistics*, vol. 1, no. 2, pp. 141–149, 1992.

[34] K. I. Park, *Fundamentals of Probability and Stochastic Processes with Applications to Communications*. Springer, 2018.

[35] Z. D. Bai and J. W. Silverstein, "Exact Separation of Eigenvalues of Large Dimensional Sample Covariance Matrices," *The Annals of Probability*, vol. 27, no. 3, pp. 1536–1555, 1999.

[36] Z. D. Bai, B. Q. Miao, and G. M. Pan, "On asymptotics of eigenvectors of large sample covariance matrix," *The Annals of Probability*, vol. 35, no. 4, pp. 1532 – 1572, 2007.

[37] Z. D. Bai and J. W.Silverstein, "CLT for Linear Spectral Statistics of Large-Dimensional Sample Covariance Matrices," *The Annals of Probability*, vol. 32, no. 1A, pp. 553–605, 2004.

[38] H. Cramér and H. Wold, "Some Theorems on Distribution Functions," *Journal of the London Mathematical Society*, vol. 1-11, no. 4, pp. 290–294, 1936.

[39] W. Hachem, O. Khorunzhiy, P. Loubaton, J. Najim, and L. Pastur, "A New Approach for Mutual Information Analysis of Large Dimensional Multi-Antenna Channels," *IEEE Transactions on Information Theory*, vol. 54, no. 9, pp. 3987–4004, 2008.

[40] M. S. L. Pastur, *Eigenvalue Distribution of Large Random Matrices*, ser. Mathematical surveys and monographs. American Mathematical Society, 2011.

[41] W. Hachem, P. Loubaton, X. Mestre, J. Najim, and P. Vallet, "Large Information Plus Noise Random Matrix Models and Consistent Subspace Estimation in Large Sensor Networks," *Random Matrices: Theory and Applications*, vol. 01, no. 02, p. 1150006, 2012.

[42] L. H. Chen, "An Inequality for the Multivariate Normal Distribution," *Journal of Multivariate Analysis*, vol. 12, no. 2, pp. 306 – 315, 1982.

[43] D. Schenck, X. Mestre, and M. Pesavento, "Probability of Resolution of MUSIC and g-MUSIC: An Asymptotic Approach," 2021. [Online]. Available: arXiv:2106.08738

[44] R. A. Horn and C. R. Johnson, *Matrix Analysis*. Cambridge; New York: Cambridge University Press, 2005.

[45] J. E. Marsden and M. J. Hoffman, *Basic Complex Analysis*. W. H. Freeman, 1999, vol. 3.